MAGNETORHEOLOGICAL CHARACTERIZATION OF MAGNETO-RESPONSIVE FLUIDS

by

Darlene Ivelisse Santiago Quiñones

A dissertation submitted in partial fulfillment of the requirements for the degree of

DOCTOR OF PHILOSOPHY
in
CHEMICAL ENGINEERING

UNIVERSITY OF PUERTO RICO
MAYAGÜEZ CAMPUS
2012

Approved by:

_____	_____
Carlos Rinaldi, Ph.D. President, Graduate Committee	Date
_____	_____
Aldo Acevedo, Ph.D. Member, Graduate Committee Acting Department Director	Date
_____	_____
Julio Briano, Ph.D. Member, Graduate Committee	Date
_____	_____
María Martinez-Iñesta, Ph.D. Member, Graduate Committee	Date
_____	_____
Dra. Danna Collins Graduate Studies Representative	Date

To my mom and my dad, Wanda and Pepe,
whose love and support have guided me through the years.
And to my husband, Anthony,
you inspire me every day to become more than I was yesterday,
I love you…

ABSTRACT

The work presented in this dissertation focuses primarily on the rheological characterization of magneto-responsive fluids, consisting of suspensions of magnetic nanoparticles in non-magnetic liquid media. The rheology of these fluids has shown to be promising due to their enhanced viscous behavior when acted upon by external magnetic fields. This enhancement occurs due to a chaining of the nanoparticles, resulting in enhanced resistance to the applied shear. The rheology of magneto-responsive fluids with applied magnetic fields presented here, also known as magnetorheology, was studied for magneto-responsive fluids such as ferrofluids, and for others were the suspending medium is a non-Newtonian fluid.

For the case of ferrofluids, we have clarified the role of the particle's magnetic relaxation mechanism and the magnetic aggregation effect on their magnetorheoloical behavior. The first study focused on two cases, a (i) rotating (Neél relaxation) and (ii) fixed (Brownian relaxation) magnetic moments and their effect on the balance between magnetic and hydrodynamic torques. The second study focused on the effect of magnetic field dependent aggregation behavior of the nanoparticles on the magnetrheology of these fluids. Magnetorheological studies of magneto-responsive non-Newtonian fluids where performed using polymer liquid crystals (ferronematics) and surfactants (magnetic surfactant solutions) as suspending media, reporting new types of magnetic soft materials. All these measurements were performed using a rheometer capable of applying magnetic fields and measuring rheological properties simultaneously such as viscosity flow curves, yield stresses, and storage and loss modulus (moduli), all magnetic field dependent.

RESUMEN

El trabajo presentado en ésta disertacion doctoral se enfoca principalmente en la caracterización reológica de fluídos que responden a campos magnéticos, los cuales consisten en suspensiones de nanopartículas magnéticas en un medio líquido no magnético. La reología de éstos fluídos ha demostrado ser prometerdora debido a su aumento en viscosidad cuando entran en contacto con un campo magnético, resultando en una resistencia a el flujo cortante aplicado. La reología de fluidos que responden a campos magnéticos presentada aquí, también conocido como magnetoreología, fue estudiada en fluídos tradicionales como ferrofluidos, y también en otros donde el medio donde se suspenden las partículas es uno no Newtoniano.

En el caso de ferrofluidos, se estudió el rol de la relajación magnética y la agregación en sus propiedades rheológicas. Primero, se estudiaron dos mecanismos de relajación magnética, (i) dipolo fijo y (ii) dipolo rotacional, y el efecto de éstos en el balance de torques magnéticos e hidrodinámicos de las partículas al aplicarle campos magnéticos y esfuerzos cortantes simultaneamente. Segundo, se estudió la agregación de partículas inducida por un campo magnético aplicado, y el efecto de ésto en el comportamiento reológico. Estudios magnetoreológicos de fluídos que responden a campos magnéticos suspendidos en un medio no Newtoniano fueron relizados utilizando polímeros (ferronematicos) y surfactantes como medios de dispersión. Todas éstas medidas fueron realizadas utilizando un reómetro capaz de aplicar campos magnéticos y medir propiedades reológicas simultáneamente. Pruebas realizadas incluyen curvas de viscosidad, y modulos de almacenamiento y perdida.

ACKNOWLEDGMENTS

First and most importantly I would like to thank God, without him I wouldn't be here. Secondly I thank my advisor Dr. Carlos Rinaldi, for giving me the opportunity of working with him, and most importantly for believing in me, even when I didn't. I want to thank Dra. Magda Latorre and (now Dra.) Sindia Rivera and Mar Creixell, I do not think that without the support of these extraordinarily exceptional and admirable women I would have achieved what I have. We were there for each other, during the bad, the good, and the ugly. Your support and knowledge has teached me today how to become a better woman scientist.

I thank my mom and dad for always supporting my career and most importantly for the moral support needed on a daily basis during the last five years. I thank my brother for inspiring me to be a better professional. I also thank my husband Anthony Gonzalez. You taught me how to be patient and to persevere on what I believed. I love you so much, thanks for always believing in me. We were there for each other, and we did it.

I would also like to thank my group mates, for their support throughout this experience. I would like to thank Roberto Olayo and Edwin de la Cruz for helping with TEM samples. Isaac Torres for the long companionship in the lab were no one wanted to be, never. Lorena Maldonado and Liliana Polo for helping me with nanoparticles synthesis. Michelle Visbal for your support with electrical related issues. Vanessa Ayala and Ana Carolina, thanks for the moral support, every day. I have to thank the last two new lab members, Dr. Jeremiah Hubbard and Dra. Lenibel Santiago, although we only spent a little time together, I am very thankful for your support and friendship, we had a great time. Finally, I thank the three women that already left our group, still they were here when I arrived, Dra. Adriana Herrera, Dra. Victoria Calero, and Dra. Carola Barrera, I learned a lot from these women, thank you. I am very grateful to the Chemical Engineering Department staff and faculty

working at UPRM. Dr. Aldo Acevedo, thank you for providing your support and mentorship throughout this process. Angel Zapata, thank you for helping with technical issues with equipments and laboratory issues. Finally I thank Anton Paar for always providing their support with the rheometer.

Table of Contents

1 Introduction and Motivation

Ferrofluids are colloidally stable relatively dilute suspensions of magnetic nanoparticles undergoing rotational and translational Brownian motion in a non-magnetic liquid carrier [1]. They are a type of magnetoresponsive fluid but should not be confused with magnetorheological fluids, which consist of micron sized magnetizable particles at much higher particle concentrations [2, 3]. Particles in ferrofluids may be permanently magnetized or magnetizable and typically range between 10 and 30 nanometers in diameter. They are surface modified to prevent aggregation due to van der Waals and magnetic interactions. The magnetic nanoparticles, typically magnetite or cobalt ferrite, may be obtained in a laboratory synthesis through different mechanisms [4, 5].

The rheology of ferrofluids has been studied experimentally since 1969 [6, 7]. This due to their interesting behavior when acted upon by a magnetic field, where a viscosity increase results. Parameters such as shear rate [8], microstructure [9], particle polydispersity [10], particle synthesis [11], and aggregation [12] have been reported, in addition to proposed custom made rheometers that are used for rheological characterization [13] with increments of almost 2 decades in viscosity [1, 11]. Higher magnetic field dependent viscosity increments (over 3 decades) have been reported for magnetorheological fluids [2, 14-16]. Additionally, the magnetorheology of MR fluids has received wider attention with demostrations of (i) power law viscosity behavior [17], (ii) magnetic field dependent storage and loss moduli [18, 19], and (iii) magnetic field dependent yield stresses [20]. On the other hand, work with ferrofluids has been limited to reporting a magnetic field dependent viscosity increase, typically with magnetite-based ferrofluids.

A tendency of studying magnetite-based ferrofluids clearly exists in the literature [1, 8, 9, 11, 13, 21-25]. This is the most commonly studied ferrofluid where magnetizable

nanoparticles are used (the magnetic dipole of the nanoparticles is not fixed) allowing free dipole rotation when magnetized (Neél magnetic relaxation). Cobalt ferrite nanoparticles have a fixed magnetic dipole, resulting in particle rotation upon application of a magnetic field (Brownian magnetic relaxation). Most prior work with ferrofluids consisted of highly polydispersed collections of nanoparticles. Because the two relaxation mechanisms possess different functional dependencies on particle size, the Néel mechanism dominates for small particles and the Brownian mechanism dominates for large particles. Polydisperse ferrofluids typically respond to magnetic fields through a complex, sample-dependent mixture of the two mechanisms. This makes it difficult to make quantitative comparisons between experiments and theoretical expectations. Thus, by focusing mostly on magnetite, prior work has at best only considered the Nèel relaxation mechanism and at worst has been confused by the fact that the particles respond through both relaxation mechanisms in a sample dependent manner.

Recent work has focused on enhancing the magnetic field dependent rheological properties of other magneto responsive fluids, so-called magnetic soft matter. These reports explore changes in the magnetic field dependent rheological properties of mixtures of magnetic fluids and additives. A comprehensive rheological behavior is studied, due to the unique rheological behavior that these soft fluids exihibit without the nanoparticles. Increasing loadings of additives to magnetic suspensions has resulted in induced yield stresses and viscoelastic behavior, along with higher measured magnetic viscosities [26-32]. However, a new breed of magnetoresponsive soft fluids where small amounts of nano sized particles lead to marked changes in the rheological properties of the suspending media has received increasing attention. Among these are ferronematics [33] and ferrogels [32, 34-39], which are dilute suspensions of nanoparticles in liquid crystals and gels and which have shown interesting enhanced rheological behavior upon application of a magnetic field.

To fill in some of the gaps present in the literature regarding the magnetorheological behavior of ferrofluids, we have designed a set of experiments with synthesized and commercial ferrofluids. We analyzed these experimental data in terms of the reported characteristic rheological response of magnetorheological fluids such as, power law viscosity behavior, magnetic field dependent viscoelastic behavior, and yield stresses. Moreover we have applied a dimensionless analysis using a modified version of the so-called Mason number (balance of viscous to magnetic energies) [40]. We show critical shear rate values where a threshold magnetic field dependent viscosity sets in due to magnetic energies dominating viscous energies. With the synthesized ferrofluids we studied the effect of the magnetic relaxation mechanism on their magnetorheological behavior. We prepared a series of samples with Neél and Brownian relaxation, with different particle loadings ranging from 0.01% to 5% v/v, and studied their magnetorheology. Additionally, we studied commercial magnetite based ferrofluids where the particle's magnetic interactions were modulated to evaluate their effect on the magnetorheology of the ferrofluid. Power law viscous behavior, viscoelasticity, and yield stresses were also investigated and analyzed. To our knowledge, these results comprise the first magnetorheological study of ferrofluids where the experimental data was analyzed in these terms. The magnetorheology of two soft magnetic materials was also investigated, a ferronematic, and a magnetic concentrated amphiphilic surfactant solution, both analyzed with respect to their power law rheological behavior, and magnetic field dependent moduli and yield stresses.

This dissertation provides improved understanding of the role of magnetic interactions, magnetic relaxation, and presence of additives in the magnetorheology of ferrofluids. The dissertation is organized as follows. Chapter 2 presents a review of the relevant literature to the dissertation. In Chapter 3 the magnetorheology of Neél and Brownian ferrofluids is presented. In Chapter 4 the magnetorheology of commercial

magnetite based ferrofluids having magnetic field dependent aggregation is presented. Chapter 5 presents the enhanced rheological behavior of a surfactant concentrated solution by means of adding small loads of magnetic nanoparticles and applied magnetic fields. Finally Chapter 6, presents the enhanced magnetic field dependent rheological behavior of a polymer liquid crystal by addition of magnetic nanoparticles.

2 Literature Review

2.1 Ferrofluids

Ferrofluids are colloidally stable relatively dilute suspensions of magnetic nanoparticles undergoing rotational and translational Brownian motion in a non-magnetic liquid carrier [1]. They should not be confused with magnetorhelogical fluids, which consist of suspensions of micron sized magnetizable particles at much higher particle concentrations [41]. Particles in ferrofluids may be permanently magnetized or magnetizable and typically range between 10 and 30 nanometers in diameter. They are surface modified to prevent aggregation due to van der Waals and magnetic attraction. The magnetic nanoparticles may be obtained in a laboratory synthesis through different routes [42, 43]. The magnetic nature of ferrofluids and their ability to respond to external magnetic and flow fields makes them attractive materials for novel research areas and applications.

2.1.1 Nanoparticle Synthesis

Several synthesis methods for magnetic nanoparticles exist, such as reverse micelles, pyrolysis, hydrothermal and electrothermal techniques, sonolysis, flow injection, co-precipitation, and thermal decomposition [43], the last two being the most commonly used techniques.

In the co-precipitation technique metal salt precursors are precipitated in an aqueous solution using NaOH or NH_4OH as precipitants [42]. This technique proves useful when large amounts of magnetic nanoparticles are required. However, it produces particles with a wide size distribution (*i.e.* polydisperse), due to lack of control of the nucleation and growth rates. In addition, particles that are obtained from the co-precipitation technique tend to be agglomerated, which causes poor colloidal stability and hence precipitation. Polydispersity

and agglomeration in ferrofluids greatly affect their physical, magnetic, and rheological properties and thus their applications.

Another technique in nanoparticle synthesis is the thermal decomposition method [44]. This method produces particles with narrow size distributions and diameters ranging from 10-20 nm. This technique consists of the decomposition of metal precursors using high boiling point solvents such as 1-octadecene, 1-hexadecene, and dioctyl ether, among others. Here the nucleation rate of the particles is controlled by a rapid increase in system temperature, causing nucleation to initiate homogenously until the net nucleation rate drops to zero. This is followed by slowly increasing the temperature to the boiling point of the solvent, which promotes the growth of the particles by diffusion of free metal atoms to the growing particles [44]. Surfactants such as oleic acid and oleylamine are used during synthesis to avoid particle agglomeration. In one variant of this technique a metal-oleate complex is formed, allowing nanocrystal growth to occur from there. The size of the magnetic nanoparticles may be tuned with variations in concentration of reagents, reaction temperature, and solvent [45].

2.1.2 Magnetic Properties of Nanoparticles

The equilibrium magnetization behavior of ferrofluids can be described using the Langevin function by taking into account the particle's lognormal size distribution [46]

$$M = \int_0^\infty M_s \left[\coth\alpha\left(H,D_m\right) - \frac{1}{\alpha\left(H,D_m\right)} \right] n_v\left(D_m\right)\, dD_m, \tag{1}$$

where M is the magnetization of the suspension at an applied magnetic field H, M_s is the saturation magnetization, $\alpha\left(H,D_m\right)$ is the Langevin parameter, and $n_v\left(D_m\right)$ is the volume

weighted lognormal distribution for the magnetic diameter D_m. The Langevin parameter is given by [46]

$$\alpha\left(H,D_m\right)=\frac{\mu_0\pi M_d H D_m^3}{6k_B T}, \tag{2}$$

where μ_0 is the permeability of free space, M_d is the domain magnetization, k_B is the Boltzman constant, and T is the sample temperature. The volume weighted lognormal distribution is given by

$$n_v\left(D_m\right)=\frac{1}{\sqrt{2\pi}D_m \ln\sigma_g}\exp\left(-\frac{\ln^2\left(D_m/D_{mgv}\right)}{2\ln^2\sigma_g}\right), \tag{3}$$

where D_{mvg} is the volume mean magnetic diameter and $\ln\sigma_g$ is the geometric deviation of the distribution.

A typical magnetization curve for a ferrofluid (Figure 1) behaves initially with the magnetization increasing linearly with the applied magnetic field, known as the linear magnetization region, followed by saturation of the magnetization, were all the magnetic dipoles of the particles are aligned in the direction of the applied magnetic field.

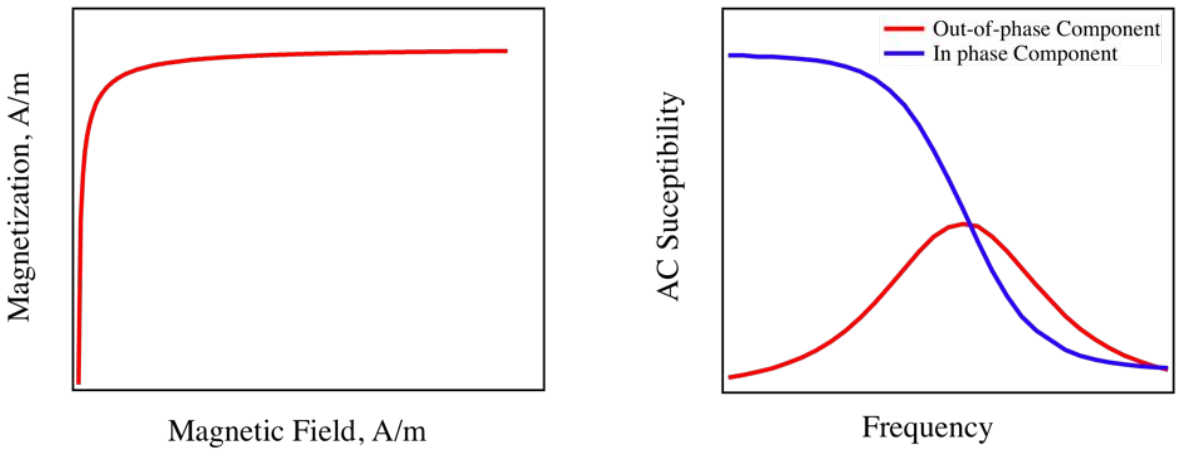

Figure 1. Typical equilibrium magnetization behavior and AC susceptibility of nanoparticles.

Application of oscillating magnetic fields to ferrofluids provides information regarding the dynamic behavior of the suspended nanoparticles. The response of the ferrofluid to oscillating magnetic fields is typically parameterized through the so-called AC susceptibility (Figure 1). When measuring AC susceptibility of materials an oscillating magnetic field is applied [47],

$$H = H_0 \cos(\omega\tau). \tag{4}$$

The magnetization response of the particles to the oscillating magnetic field is given by [47],

$$M(t) = H_o(\chi' \cos\omega t + \chi'' \sin\omega t). \tag{5}$$

where χ' and χ'' are the in-phase and out-of-phase components of the complex susceptibility, $\hat{\chi} = \chi' - i\chi''$ [47],

$$\chi' = \frac{\chi_0}{1+(\omega\tau)^2} \quad ; \quad \chi'' = \frac{\omega\tau}{1+(\omega\tau)^2}\chi_0. \tag{6}$$

In (8) χ_0 is the initial susceptibility and τ is the characteristic magnetic relaxation time of the particles. The magnetic relaxation time is the characteristic time it takes for the magnetic dipole of a particle to align in the direction of the applied magnetic field. The in-phase and out-of-phase components of the complex susceptibility are typically plotted as a function of the applied field frequency (Figure 1). The in-phase and out-of-phase susceptibilities cross at the peak of the out-of-phase susceptibility, where $\omega\tau = 1$. This allows calculation of the relaxation time of the particles [48].

There are two mechanisms by which magnetic nanoparticles align to applied magnetic fields, Néel and Brownian relaxation. In the Néel mechanism only the internal magnetic dipole of the particle rotates and aligns in the direction of the applied field without physical particle rotation. The Neél relaxation time is,

$$\tau_N = \frac{1}{f_0} exp\left(\frac{KV}{k_B T}\right) \tag{7}$$

where f_0 is the Larmour frequency of the magnetization ($f_0 = 10^9 s^{-1}$) [46], K is the anisotropy constant of the particles, V is the volume of the particle, k_B is Boltzman's constant, and T is the absolute temperature. On the other hand, in the Brownian relaxation mechanism the magnetic dipoles of the particles are fixed in a crystal direction, thus, there is physical rotation and alignment of the particles in the direction of the applied magnetic field. The characteristic Brownian relaxation time is given by,

$$\tau_B = \frac{3\eta_0 V_h}{k_B T} \tag{8}$$

where η_0 is the solvent viscosity and V_h is the hydrodynamic volume of the nanoparticles. It should be noted that Néel magnetic relaxation depends on the magnetic core volume of the nanoparticles whereas in the Brownian mechanism the relaxation depends on the hydrodynamic volume. Particles that relax through the Néel mechanism can be considered as magnetizable particles, whereas those that relax through the Brownian mechanism can be considered as permanently magnetized nanoparticles. The relaxation mechanism in a suspension will follow the process with the shortest relaxation time. Equations (7) and (8) show that the relaxation time of magnetic nanoparticles increases with particle size, τ_B increases in a cubic relation with diameter, while τ_N increases exponentially with the cube of particle diameter. Thus for relatively small particles the Brownian relaxation time will be larger than the Néel relaxation time, and relaxation will take place by rotation of the internal moment of the particles (Neél mechanism). The converse is true for large particles.

2.1.3 Particle Chaining Phenomena

When a magnetic field is applied to a ferrofluid, clustering or chaining of particles results due to the magnetic dipole-dipole interactions between the particles, evidenced in

some ferrofluids by microscopy and scattering techniques [49, 50]. Chain formation in turn affects other physical properties of ferrofluids, such as their rheological behavior [46].

The first theoretical expressions for the formation of chains of colloidal magnetic particles under the influence of a magnetic field were reported by de Gennes [51] and Jordan [52]. These expressions were based on the properties of a "ferromagnetic gas" suspended in an inert liquid. The relative orientation of magnetic dipoles under the influence of a magnetic field will be highly constrained whenever they are close enough to interact. Jordan [52] and de Gennes [53] independently demonstrated that for an isolated pair of interacting particles, they would most likely exist near the distance of closest approach with their magnetic dipoles aligned nearly parallel.

For linear chains of particles with an external magnetic field arranged parallel to the chain one may obtain the mean number of particles per chain [46],

$$n_{\infty} = \left[1 - \frac{2}{3}\left(\frac{\phi}{\lambda^2}\right)e^{2\lambda}\right]^{-1} \tag{9}$$

where ϕ is the volumetric fraction of the suspended particles and λ is the dimensionless interaction parameter, defined as,

$$\lambda = \frac{\mu_0 m^2 V}{24kT} \tag{10}$$

where μ_0 is the free space permeability, m is the magnetic moment of the particles, V is the volume, and kT is the thermal energy. This interaction parameter is commonly used to quantify the strength of magnetic particle-particle interactions. In the absence of an applied magnetic field, and with low particle interactions $(0 < \lambda << 1)$, there exists, according to predictions [46], a number of particles per chains given by,

$$n_0 = \left[1 - \frac{2}{3}\left(\frac{\phi}{\lambda^3}\right)e^{2\lambda}\right]^{-1}. \tag{11}$$

Here the number of chains would be smaller than with an applied magnetic field. These equations for the number of magnetic particles in a chain with and without magnetic fields were developed for magnetizable particles (Néel type relaxation) by deGennes [51]. The interaction parameter is still used today when studying particle-particle interactions in Néel type ferrofluids theoretically [15, 54-57] and experimentally [1, 25].

The theory of de Gennes and Jordan for chaining of particles is still used today to interpret phenomena in ferrofluids in external magnetic fields. This particle chaining has been demonstrated experimentally [1, 58-61], theoretically [12, 54, 62, 63], and with simulations [64-67]. This chaining behavior has been reported in ferrofluids consisting of magnetite [68], maghemite [69] and iron [70] nanoparticles. They all coincide in that for ferrofluids with moderate to strong dipole-dipole interactions the most probable structural arrangement when in a magnetic field would be chains of particles.

2.1.4 Magnetorheological Behavior of Ferrofluids

Application of magnetic fields to a ferrofluid subjected to shear deformation results in interesting rheological behavior. Alignment of the particle's magnetic dipole in the direction of the applied magnetic field results in a viscosity enhancement of the ferrofluid, also known as the "magnetoviscous effect" [1].

The first experimental investigation of the magnetic field effect in the viscosity of a dilute ferrofluid was reported by McTague in 1969 [71]. The ferrofluid consisted of cobalt ferrite nanoparticles of ~6nm with an assumed Brownian relaxation mechanism which showed an increase in viscosity with applied magnetic fields normal to the flow. The fluid's viscosity was measured in a capillary viscometer with an attached permanent magnet. Subsequently Hall and Busenberg [7] reported a theoretical approach for the magnetic field

effect on the viscosity of a dilute magnetizable ferrofluid with magnetic field applied parallel and normal to the shear deformation. Here an expression was obtained for the viscosity neglecting Brownian relaxation motion of the particles which is similar to Einstein's,

$$\eta_{(H)} = \eta_0\left(1 + \frac{5}{2}\tilde{\phi} + \frac{3}{2}\phi' \sin^2\varepsilon\right), \tag{12}$$

where $\tilde{\phi}$ is the volume concentration of the particles, ϕ' is the volume fraction of the particles. The magnetic contribution is incorporated in the $\sin^2\varepsilon$ term which is,

$$\sin^2\varepsilon = \frac{1}{2}\left(1+\xi^{-2}\right) - \left[\frac{1}{4}\left(1+\xi^{-2}\right) - \left(\xi^{-2}\sin^2\beta\right)\right]^{\frac{1}{2}} \;\; ; \;\; \xi^{-2} = \frac{\mu_0 m H}{4\pi\eta_0 d^3\dot{\gamma}} \tag{13}$$

where β is the angle between the flow vorticity and the magnetic field direction, ξ represents the ratio between the magnetic and viscous torques acting on the particles, μ_0 is the vacuums permeability, m is the magnetic moment of the particles, H is the applied magnetic field, η_0 is the fluids viscosity, d is the particles diameter, and $\dot{\gamma}$ is the applied shear deformation.

This was followed by Rosensweig and co-workers [6] who studied the effect of shear rate effect on the viscosity of a ferrofluid consisting of magnetite particles of 72 to 136 Å in diameter. Their approach was to study the variables that affect the rheological properties of four magnetite based ferrofluids with different solvents under magnetic fields. They worked under the assumption that the magnetic particles were non-interacting and monodisperse. Shear thinning behavior with magnetic fields was reported for the first time, and a scaling analysis allowed a collapse of the data.

Rosensweig and co-workers were first to report a dimensionless number describing the magnetic field effect on the rheology of ferrofluids. This number, which they called a "stress tensor", is given by:

$$ST = \frac{\dot{\gamma}\eta_0}{MH} \tag{14}$$

where η_0 is the solvent's viscosity, M is the particle's magnetization, and H is the applied magnetic field. It described the ratio of shear to magnetic forces by collapsing the magnetorheological data of the ferrofluids studied.

The magnetoviscous effect was described theoretically by Shliomis [72] in 1972. He incorporated Brownian motion of the particles into derivations using the ferrohydrodynamic equation which integrates magnetic and viscous contributions to the fluid's response with an equation for the relaxation of the internal angular momentum of a particle under shear and magnetic deformations in a Couette planar flow. The following expression was obtained,

$$\eta_m = \frac{3}{2}\phi'\eta_0 \frac{\alpha - \tanh\alpha}{\alpha + \tanh\alpha}\left\langle \sin^2\beta \right\rangle \quad ; \quad \alpha = \frac{\mu_0 mH}{kT} \tag{15}$$

Here ϕ' is the hydrodynamic volume fraction of the particles, η_0 is the carrier fluid's viscosity, μ_0 is the vacuum permeability, m is the magnetic moment of the particles, β is the angle between the magnetic field and the vorticity, H is the applied magnetic field, k is the Boltzman constant, and T is the sample temperature.

Shliomis' derivation was for dilute ferrofluids, where magnetic dipole interactions between particles are negligible. This theory predicts that the viscosity enhancement of a ferrofluid is due to the hindrance of rotation of individual particles, primarily dominated by the thermal motion of the particles. Shliomis considered a single particle model where the hydrodynamics of one particle does not affect its nearest neighbors. Viscosity increments with applied magnetic fields in dilute ferrofluids with no magnetic dipole interactions result in only a few percentage changes in viscosity. For higher changes in viscosity to be obtained the particle concentration must be increased, therefore particle-particle interactions become important.

The magnetorheology of ferrofluids has been reported by various authors [9, 11, 22, 23, 54, 73]. Odenbach and co-workers have made numerous studies, mostly of commercial magnetite ferrofluids using a custom made cone and plate rheometer that applied magnetic fields while measuring the rheological properties of ferrofluids [13]. In their work, commercial ferrofluids obtained from FERROFLUIDICS with particles of approximately 10 nm obtained via the co-precipitation method and at concentrations of 7 vol% were typically used. Their studies show the increase in viscosity of the ferrofluids with applied magnetic fields normal to the flow direction. Odenbach and co-workers attributed the increase in viscosity to chain like structures of particles that arise upon contact with a magnetic field, later demonstrated by small angle neutron scattering [9]. This enhanced viscosity could not be described with classical theories of rotational viscosity, much less with concentrated fluids at low shear rates where magnetic interactions are present.

Although seminal to the field, Odenbach's work possesses some limitations. The applied shear rate range was limited to only one decade. Limiting shear rate measurements results in a limited anlysis of the viscosity behavior of the ferrofluids. In addition, the ferrofluids studied by Odenbach were mostly magnetite based ferrofluids with aggregated and highly polydisperse particles. Perhaps the most important observation of Odenbach work is the subtle viscosity increase with the applied magnetic fields attributed to chain formation the particles when acted upon by a magnetic field.

Recently the work of Ghasemi [11] and Hong [21] on magnetorheology of ferrofluids showed a more pronounced effect with over two decades increase of the viscosity of the ferrofluid. Again magnetite-based ferrofluids were used. Ghasemi and co-workers reported shear thinning of the ferrofluid without magnetic fields and with three decades in viscosity change, indicating strong magnetic interactions between particles. Moreover they studied a wide range of shear rates, ranging from 0.1 to 1000 s^{-1}. As magnetic fields were applied, an

increase in viscosity of one order of magnitude resulted with an applied magnetic field of 90 kAm^{-1}.

As summarized, recent experimental work on the magnetorheology of ferrofluids, although significant, has failed to capture important and fundamental elements. Magnetic field dependent viscosity increase has been vastly reported. However other interesting magnetorheological behavior has not, such as magnetic field dependent viscoelastic response of the fluid, due to the chain formation when the particles are acted upon by a magnetic field. These chains of particles may also induce magnetic field dependent yield stresses due to a combination of magnetic and elastic forces acting by the fluid. All these, reported for other magnetoresponsive fluids such as magnteorheological fluids (MRFs), have not been reported in ferrofluids. In the following chapters, four studies performed in order to fill some of these gaps will be described. Starting first with a comprehensive study of the magnetic relaxation effect of the nanoparticles on the magnetoviscous effect of the ferrofluids analized in terms of (i) power law viscous behavior, (ii) magnetic field dependent moduli and (iii) magnetic field dependent yield stress (Chapter 3). Followed by a study of the magnetorheology of a magnetic field dependent aggregation behavior of commercial magnetite-based ferrofluids, again studied by means of (i) power law viscous behavior, (ii) magnetic field dependent moduli and (iii) magnetic field dependent yield stress (Chapter 4). This is followed by a study focusing on enhanced rheological properties of surfactant amphiphilic based concentrated solutions by addition of small particle loadings and by application of magnetic fields (Chapter 5). Finally, we studied the enhanced magnetic field dependent viscous behavior of polymer based liquid crystals by incorporating magnetic nanoparticles in their crystalline structure (Chapter 6).

References

1. Odenbach, S., *Magnetoviscous Effects in Ferrofluids.* 2002, Berlin: Springer.
2. de Vicente, J., D.J. Klingenberg, and R. Hidalgo-Alvarez, *Magnetorheological fluids: a review.* Soft Matter. **7**(8): p. 3701-3710.
3. Bossis, G., et al., *Magnetorheogical fluids.* Journal of Magnetism and Magnetic Materials, 2002. **252**: p. 224-228.
4. Sun, S.H. and C.B. Murray, *Synthesis of monodisperse cobalt nanocrystals and their assembly into magnetic superlattices (invited).* Journal of Applied Physics, 1999. **85**(8): p. 4325-4330.
5. Herrera, A.P., C. Barrera, and C. Rinaldi, *Synthesis and functionalization of magnetite nanoparticles with aminopropylsilane and carboxymethyldextran.* Journal of Materials Chemistry, 2008. **18**(31): p. 3650-3654.
6. Rosensweig, R., R. Kaiser, and G. Miskolcz, *Viscosity of Magnetic Fluid in a Magnetic Field.* Journal of Colloid and Interface Science, 1969. **29**(4): p. 680-&.
7. Hall, W.F. and S.N. Busenberg, *Viscosity of Magnetic Suspensions.* The Journal of Chemical Physics, 1969. **51**(1): p. 137-144.
8. Odenbach, S. and H. Stork, *Shear dependence of field-induced contributions to the viscosity of magnetic fluids at low shear rates.* Journal of Magnetism and Magnetic Materials, 1998. **183**: p. 188-194.
9. Pop, L., et al., *Microstructure and rheology of ferrofluids.* Journal of Magnetism an Magnetic Materials, 2005. **289**: p. 303-306.
10. de Gans, B.J., et al., *The influence of particle size on the magnetorheological properties of an inverse ferrofluid.* Journal of Chemical Physics, 2000. **113**(5): p. 2032-2042.

11. Ghasemi, E., A. Mirhabibi, and M. Edrissi, *Synthesis and rheological properties of an iron oxide ferrofluid.* Journal of Magnetism and Magnetic Materials, 2008. **320**(21): p. 2635-2639.

12. Ivanov, A.O. and S.S. Kantorovich, *Chain aggregate structure and magnetic birefringence in polydisperse ferrofluids.* Physical Review E, 2004. **70**(2): p. 10.

13. Odenbach, S., T. Rylewicz, and M. Heyen, *A rheometer dedicated for the investigation of viscoelastic effects in commercial magnetic fluids.* Journal of Magnetism and Magnetic Materials, 1999. **201**: p. 155-158.

14. Zubarev, A.Y., *Theory of magnetic fluids with chain aggregates.* Magnetohydrosynamics, 1992. **28**(1).

15. Zubarev, A.Y., *Rheological properties of polydisperse magnetic fluids. Effect of chain aggregates.* Journal of Experimental and Theoretical Physics, 2001. **93**(1): p. 80-88.

16. Klingenberg, D., J. Ulicny, and M. Golden, *Mason number for magneorheology.* Journal of Rheology, 2007. **51**(5): p. 883-893.

17. Felt, D.W., et al., *Rheology of a Magnetorheological Fluid.* Journal of Intelligent Material Systems and Structures, 1996. **7**: p. 589-593.

18. Ramos, J., J. de Vicente, and R. Hidalgo-Alvarez, *Small-Amplitude Oscillatory Shear Magnetorheology of Inverse Ferrofluids.* Langmuir. **26**(12): p. 9334-9341.

19. Weiss, K.D., J.D. Carlson, and D.A. Nixon, *VISCOELASTIC PROPERTIES OF MAGNETORHEOLOGICAL AND ELECTRORHEOLOGICAL FLUIDS.* Journal of Intelligent Material Systems and Structures, 1994. **5**(6): p. 772-775.

20. Tang, X., et al., *Structure-enhanced yield stress of magnetorheological fluids.* Journal of Applied Physics, 2000. **87**(5): p. 2634-2638.

21. Hong, R.Y., et al., *Rheological properties of water-based Fe3O4 ferrofluids.* Chemical Engineering Science, 2007. **62**(21): p. 5912-5924.

22. Odenbach, S., *Ferrofluids, Magnetically Controllable Fluids and Their Applications*. 1 ed. 2002, Berlin: Springer.

23. Odenbach, S., *Ferrofluids - magnetically controlled suspensions.* Colloids and Surfaces a-Physicochemical and Engineering Aspects, 2003. **217**(1-3): p. 171-178.

24. Pop, L.M., et al., *The microstructure of ferrofluids and their rheological properties.* Applied Organometallic Chemistry, 2004. **18**(10): p. 523-528.

25. Pop, L.M. and S. Odenbach, *Investigation of the microscopic reason for the magnetoviscous effect in ferrofluids studied by small angle neutron scattering.* Journal of Physics-Condensed Matter, 2006. **18**(38): p. S2785-S2802.

26. Ginder, J.M., et al., *Magnetostrictive phenomena in magnetorheological elastomers.* International Journal of Modern Physics B, 2002. **16**(17-18): p. 2412-2418.

27. Ginder, J.M., L.C. Davis, and L.D. Elie, *Rheology of magnetorheological fluids: Models and measurements.* International Journal of Modern Physics B, 1996. **10**(23-24): p. 3293-3303.

28. Ginder, J.M., et al., *Magnetorheological elastomers: Properties and applications*, in *Smart Structures and Materials 1999: Smart Materials Technologies*, M. Wuttig, Editor. 1999. p. 131-138.

29. Mitsumata, T. and S. Ohori, *Magnetic polyurethane elastomers with wide range modulation of elasticity.* Polymer Chemistry. **2**(5): p. 1063-1067.

30. Xu, Y.G., et al., *A high-performance magnetorheological material: preparation, characterization and magnetic-mechanic coupling properties.* Soft Matter. **7**(11): p. 5246-5254.

31. Zrinyi, M., *Colloidal particles that make smart polymer composites deform and rotate.* Colloids and Surfaces a-Physicochemical and Engineering Aspects. **382**(1-3): p. 192-197.

32. Zrinyi, M., L. Barsi, and A. Buki, *Ferrogel: a new magneto-controlled elastic medium.* Polymer Gels and Networks, 1997. **5**(5): p. 415-427.

33. Santiago-Quinones, D.I., A. Acevedo, and C. Rinaldi, *Magnetic and magnetorheological characterization of a polymer liquid crystal ferronematic.* Journal of Applied Physics, 2009. **105**(7): p. 3.

34. Bhargavi, R., et al., *Enhanced Frank elasticity and storage modulus in a diamagnetic liquid crystalline ferrogel.* Soft Matter.

35. Gollwitzer, C., et al., *Measuring the deformation of a ferrogel sphere in a homogeneous magnetic field.* Journal of Chemical Physics, 2008. **128**(16).

36. Liu, T.Y., et al., *Study on controlled drug permeation of magnetic-sensitive ferrogels: Effect of Fe3O4 and PVA.* Journal of Controlled Release, 2008. **126**(3): p. 228-236.

37. Raikher, Y.L. and V.V. Rusakov, *Viscoelastic ferrogel: Dynamic magnetic susceptibilities.* Brazilian Journal of Physics, 2001. **31**(3): p. 366-379.

38. Ramanujan, R.V. and L.L. Lao, *The mechanical behavior of smart magnet-hydrogel composites.* Smart Materials & Structures, 2006. **15**(4): p. 952-956.

39. Snyder, R.L., V.Q. Nguyen, and R.V. Ramanujan, *Design parameters for magneto-elastic soft actuators.* Smart Materials & Structures, 2010. **19**(5).

40. Marshall, L., C.F. Zukoski, and J.W. Goodwin, *Effects of electric-fields on the rheolofy of non-aqueous concentrated suspensions.* Journal of the Chemical Society-Faraday Transactions I, 1989. **85**: p. 2785-2795.

41. Ramos, J., et al., *Steady shear magnetorheology of inverse ferrofluids.* Journal of Rheology, 2011. **55**(1): p. 127-152.

42. Massart, R., *Preparation of aqueous magnetic liquids in alkaline and acidic media.* IEE Transactions and Magnetics, 1981. **17**: p. 1247-1248.

43. Wu, W., Q. He, and C. Jiang, *Magnetic iron oxide nanoparticles: synthesis and surface functionalization strategies.* 2008. **3**: p. 397-415.

44. Park, J., et al., *Synthesis of monodisperse spherical nanocrystals.* Angewandte Chemie, 2007. **46**: p. 4630-4660.

45. Calero-DdelC, V.L.C.-D.V.L., D.I. Santiago-Quinonez, and C. Rinaldi, *Quantitative nanoscale viscosity measurements using magnetic nanoparticles and SQUID AC susceptibility measurements.* Soft Matter. **7**(9): p. 4497-4503.

46. Rosensweig, R.E., *Ferrohydrodynamics*. 1997, New York: Dover Publications, Inc.

47. Rosensweig, R.E., *Heating magnetic fluid with alternating magnetic field.* Journal of Magnetism and Magnetic Materials, 2002. **252**(1-3): p. 370-374.

48. Fannin, P.C., B.K.P. Scaife, and S.W. Charles, *The Measurement of the Frequency-dependent Susceptibility of Magnetic Colloids.* Journal of Magnetism and Magnetic Materials, 1988. **72**(1): p. 95-108.

49. Hayes, C.F., *OBSERVATION OF ASSOCIATION IN A FERROMAGNETIC COLLOID.* Journal of Colloid and Interface Science, 1975. **52**(2): p. 239-243.

50. Butter, K., et al., *Direct observation of dipolar chains in ferrofluids in zero field using cryogenic electron microscopy.* Journal of Physics-Condensed Matter, 2003. **15**(15): p. S1451-S1470.

51. Degennes, P.G. and P.A. Pincus, *PAIR CORRELATIONS IN A FERROMAGNETIC COLLOID.* Physik Der Kondensiterten Materie, 1970. **11**(3): p. 189-&.

52. Jordan, P.C., *FIELD-DEPENDENT CHAIN FORMATION BY FERROMAGNETIC COLLOIDS.* Molecular Physics, 1979. **38**(3): p. 769-780.

53. Degennes, P.G. and P.A. Pincus, *Pair Correlations In a Ferromagnetic Colloid.* Physik Der Kondensiterten Materie, 1970. **11**(3): p. 189-+.

54. Zubarev, A.Y. and L.Y. Iskakova, *On the theory of rheological properties of magnetic suspensions.* Physica a-Statistical Mechanics and Its Applications, 2007. **382**(2): p. 378-388.

55. Wang, Z.W., C. Holm, and H.W. Muller, *Molecular dynamics study on the equilibrium magnetization properties and structure of ferrofluids.* Physical Review E, 2002. **66**(2): p. 13.

56. Wang, A.R., J. Li, and R.L. Gao, *The structural force arising from magnetic interactions in polydisperse ferrofluids.* Applied Physics Letters, 2009. **94**(21): p. 3.

57. Pshenchnikov, A.F. and A.A. Fedorenko, *Chain-like aggregates in magnetic fluids.* Journal of Magnetism and Magnetic Materials, 2005. **292**: p. 332-344.

58. Lee, W.K., *X-ray microtomography of field-induced macro-structures in a ferrofluid.* Journal of Magnetism and Magnetic Materials. **322**(17): p. 2525-2528.

59. Pyanzina, E., et al., *How to analyse the structure factor in ferrofluids with strong magnetic interactions: a combined analytic and simulation approach.* Molecular Physics, 2009. **107**(4-6): p. 571-590.

60. Donselaar, L.N., et al., *Visualisation of particle association in magnetic fluids in zero-field.* Journal of Magnetism and Magnetic Materials, 1999. **201**: p. 58-61.

61. Klokkenburg, M., et al., *Quantitative real-space analysis of self-assembled structures of magnetic dipolar colloids.* Physical Review Letters, 2006. **96**(3): p. 4.

62. Ivanov, A.O., *The aggregation of ferrocolloids in a magnetic field.* Colloid Journal, 2004. **66**(6): p. 688-695.

63. Ivanov, A.O., Z.W. Wang, and C. Holm, *Applying the chain formation model to magnetic properties of aggregated ferrofluids.* Physical Review E, 2004. **69**(3): p. 6.

64. Kantorovich, S., J.J. Cerda, and C. Holm, *Microstructure analysis of monodisperse ferro fluid monolayers: theory and simulation.* Physical Chemistry Chemical Physics, 2008. **10**(14): p. 1883-1895.

65. Lomba, E., F. Lado, and J.J. Weis, *Structure and thermodynamics of a ferrofluid monolayer.* Physical Review E, 2000. **61**(4): p. 3838-3849.

66. Camp, P.J. and G.N. Patey, *Structure and scattering in colloidal ferrofluids.* Physical Review E, 2000. **62**(4): p. 5403-5408.

67. Aoshima, M. and A. Satoh, *Two-dimensional Monte Carlo simulations of a polydisperse colloidal dispersion composed of ferromagnetic particles for the case of no external magnetic field.* Journal of Colloid and Interface Science, 2004. **280**(1): p. 83-90.

68. Melle, S., et al., *Microstructure evolution in magnetorheological suspensions governed by Mason number.* Physical Review E, 2003. **68**(4): p. 11.

69. Lalatonne, Y., J. Richardi, and M.P. Pileni, *Van der Waals versus dipolar forces controlling mesoscopic organizations of magnetic nanocrystals.* Nature Materials, 2004. **3**(2): p. 121-125.

70. Erne, B.H., et al., *Rotational diffusion in iron ferrofluids.* Langmuir, 2003. **19**(20): p. 8218-8225.

71. McTague, J., *Magnetoviscosity of Magnetic Colloids.* The Journal of Chemical Physics, 1969. **51**(1): p. 133136.

72. Shliomis, M.I., *Effective Viscosity of Magnetic Suspensions.* Soviet Physics Jetp-Ussr, 1972. **34**(6): p. 1291.

73. Ivanov, A.O. and S.S. Kantorovich, *Structure of Chain Aggregates in Ferrocolloids.* Colloid Journal, 2003. **65**(2): p. 166-176.

3 Magnetorheology of ferrofluids with Neél and Brownian relaxation.

3.1 Abstract

Iron oxide and cobalt ferrite based ferrofluids were prepared with particle content ranging from 0.01 to 5% v/v, suspended in mineral oil. AC susceptibility measurements demonstrated that the cobalt ferrite ferrofluids had Brownian relaxation whereas the iron oxide ferrofluids had Neél relaxation. Their magnetic field dependent rheological properties were measured and compared, resulting in similar magnetic field viscosity increase (shear thinning) following power law behavior with slopes ranging from 0.5 to 0.91. Treatment of the data with the Mason number showed reasonable collapse for the iron oxide samples. These were collapsed first individually, showing two distinct although continuous behaviors, (i) a high shear rate Plateau (low concentrations) and (ii) a shear rate dependent viscosity decrease (higher concentrations), the latter following η/η_∞ proportional to Mn^{Δ} with $0.7 > \Delta > 0.9$. Using a scaled Mason, $Mn = Mn/Mn^{*}(\phi)$ all iron oxide data collapsed to a single curve, with slope of 0.9. Cobalt ferrite ferrofluids showed poor collapse when analyzed in this way, although, thinning behavior was observed with different power law slopes. Iron oxide ferrofluids showed magnetic field induced yield stress of up to 40 Pa whereas cobalt ferrite showed yield stresses of up to 10 Pa. The samples also showed viscoelastic behavior with magnetic field dependent viscous and storage moduli.

3.2 Figure List

3.3 Table List

3.4 Introduction

Ferrofluids (FFs) are colloidal suspensions of magnetic nanoparticles that show reversible enhanced rheological properties upon application of magnetic fields [1]. The nanoparticles in the ferrofluid undergo rotational and translational Brownian motion. Particles typically consist of single crystalline domains, with diameters between 5-15 nm, and at concentrations of up to 10%v/v. The nanoparticles in ferrofluids are typically magnetite (Fe_2O_3), with surfaces modified to improve suspension in solvents such as water and organic solvents, etc. FFs should not be confused with magnetorheological fluids (MRFs), the latter being suspensions of micron-sized multi domain magnetic particles in a non-magnetic liquid carrier.

Under the influence of an applied magnetic field the nanoparticle's magnetic moments align in the direction of the field through one of two mechanisms, Néel or Brownian relaxation. In the Néel mechanism only the internal magnetic dipole of the particle rotates and aligns in the direction of the applied field, without physical particle rotation. In the Brownian mechanism the magnetic dipoles of the particles are fixed in a crystal direction, thus, there is physical rotation and alignment of the particles in the direction of the applied magnetic field. Magnetite (Fe_3O_4) nanoparticles, which are most commonly used in ferrofluids [2-9], typically show Néel magnetic relaxation, whereas cobalt ferrite ($CoFe_2O_4$) nanoparticles relax through the Brownian mechanism.

Application of magnetic fields to a FF subjected to shear deformation results in interesting rheological behavior. Alignment of the particle's magnetic dipoles in the direction of the applied magnetic field results in a viscosity enhancement of the

ferrofluid, also known as the "magnetoviscous effect" [1]. In Brownian ferrofluids, that is ferrofluids with particles which relax solely by the Brownian mechanism, this increase in viscosity occurs due to the hindrance of the particle's rotation relative to the local vorticity, owing to a balance between the opposing magnetic and hydrodynamic torques on the particle [10]. This mechanism of viscosity increase is absent in ferrofluids with nanoparticles that relax solely through the Néel mechanism because the rotation of their magnetic dipole is uncoupled from their physical rotation. Additionally, in many ferrofluids a change in viscosity results due to formation of particle aggregates, which arise from magnetic dipole-dipole interactions between particles. The change in viscosity is then due to formation of structures that dissipate the energy of the flow, with this effect being governed by the balance between magnetic interactions keeping the structures together and hydrodynamic interactions breaking them apart.

Various authors have studied the magnetorheology of magnetite based ferrofluids. Odenbach and co-workers developed a custom rheometer to study the magnetoviscous effect in a cone-and-plate geometry [11] and used this to characterize various magnetite-based ferrofluids prepared by the co-precipitation method [1, 3, 4, 11]. They reported increments in viscosity of approximately 50% with magnetic fields of up to 30 kAm^{-1} but they were limited to two decades of shear rate ranging from approximately 1 to 100 s^{-1}. The increase in viscosity was attributed to formation of chain-like structures that arise under magnetic fields. The formation of chain-like structures was confirmed by small angle neutron scattering [7]. Recently, the work of Hong and Ghasemi also report the magnetoviscous effect in magnetite based ferrofluids, showing viscosity changes over three orders of magnitude with magnetic fields using a wider shear rate range of four

decades ranging from approximately 0.1 to 1000 s^{-1} [9, 12]. On the other hand, the magnetoviscous effect in cobalt ferrite based ferrofluids has been the subject of fewer reports [13], moreover their Brownian relaxation was not evidenced. Yield stresses have been reported in commercial Brownian and Neél ferrofluids of up to 0.07 Pa with approximately 80 kA/m [13]. Viscoelastic response in ferrofluids has been the subject of only one report [14].

Strong shear can break aggregates of magnetic nanoparticles due to the competition between magnetic and viscous forces, resulting in a decrease in the number of particles per chain with increasing shear rate and thus in shear thinning [4]. At low applied shear rates the structures are nearly undeformed, resulting in high resistance to the flow and hence an increased viscosity. As the applied shear rate increases the structures break due to viscous forces pulling particles apart. At low shear rates one could expect a plateau in viscosity due to negligible deformation of chains, whereas at very high shear rates another plateau is expected due to complete break-up of chains and structures. Odenbach and co-workers have reported a decrease of almost 80% of the enhanced viscosity in mostly magnetite-based ferrofluids [2, 9], while Ghasemi reported a broad shear thinning region with a drop of three orders of magnitude in the viscosity of magnetite based ferrodluids [12].

Most prior work seeking to describe the effect of magnetic fields and shear rate on the rheology of field responsive fluids has focused on MRFs, which show a power-law dependence between the measured viscosity and the applied shear rate, with η proportional to $\dot{\gamma}^{-\Delta}$. Martin and Anderson predicted a value of $\Delta = 1$ using a micromechanical chain-like model balancing magnetostatic and hydrodynamic forces

[15]. A value of $\Delta = 2/3$ was proposed by Halsey and co-workers who considered chain-like interactions of the particles in an electrorheological fluid (the electric field responsive analog of a MRF) and balanced magnetostatic and hydrodynamic torques. However their experimental measurements showed values of $\Delta = 0.68 - 0.93$ [16]. For inverse FFs, which serve as models for studying the magnetorheology of MRFs, De Gans [17] and co-workers reported Δ values ranging from 0.8 to 0.9, while Volkova and co-workers [18] reported values between 0.74 and 0.83. Zubarev and Iskakova [19] reported values of 0.74 and 0.767 based on their proposed theoretical model and experimental data, respectively, for inverse FFs also. Most recently Ramos and co-workers [20] reported values between 0.65 and 0.72. It is interesting that although this type of analysis has been widely applied to describe the magnetorheology of MRFs and inverse FFs, it has received little attention in the description of the mangetoviscous effect in FFs.

Due to the large number of parameters involved (e.g., magnetic field, shear rate, particle magnetization, characteristic relaxation time, etc.) and the potential complexity of their rheological behavior, dimensional analysis is attractive and potentially useful in understanding magnetic field and shear rate effects on the rheology of magnetic fluids. A dimensionless number typically used to describe the balance of viscous and magnetic forces is the Mason number (Mn). Using the Mason number to analyze experimental data allows for fewer experiments to be performed in order to explore the contributions of a large number of variables on the viscosity of the magnetic fluid. Marshall and co-workers [21] collapsed experimental flow curves of electric field responsive fluids using a proposed Mason number. An analogous Mn for magnetic field responsive fluids was reported by Volkova [18],

$$Mn = \frac{8\,\eta_0\,\dot{\gamma}}{2\mu_0\mu_f\beta^2H^2} \quad \textbf{(1)}$$

where η_0 is the carrier liquid viscosity, $\dot{\gamma}$ is the applied shear rate, μ_0 is the free space permeability, μ_f carrier fluid permeability, $\beta = (\alpha - 1)/(\alpha + 2)$ where α is the relative permeability, and H is the applied field. Later, an alternative Mason number was obtained for MRFs which accounted for magnetic saturation [22]. Typically, as the Mason number increases aggregates break leading to a viscosity that decreases with Mn [23].

Marshall [21] also introduced the concept of a critical Mn number, in analogy to the Bingham plastic constitutive equation, to collapse data obtained with electro responsive fluids of different particle fractions ϕ,

$$\frac{\eta}{\eta_\infty} = 1 + \frac{Mn^*(\phi)}{Mn} \quad \textbf{(2)}$$

where $Mn^*(\phi)$ is the critical Mn number corresponding to the transition from magnetic to hydrodynamic control of the suspension. Marshall proposed that the reduced viscosity was proportional to Mn^{-1} [15]. However, de Gans [24] reported $\eta/\eta_\infty \propto Mn^{0.8-0.9}$; Volkova and co-workers [18] $\eta/\eta_\infty \propto Mn^{0.74-0.87}$; Zubarev and co-workers [19], $\eta/\eta_\infty \propto Mn^{0.7}$; and Ramos and co-workers [20], $\eta/\eta_\infty \propto Mn^{0.76}$.

Herein we present results from an investigation of the effects of magnetic field and shear rate on the rheology of ferrofluids consisting of particles that respond to magnetic fields through Néel and Brownian relaxation. Prior work [1, 25, 26] has dealt with ferrofluids consisting of polydisperse particles that relax through a combination of both Brownian and Neél relaxation mechanisms. Particle concentrations in both FFs

varied over three orders in magnitude. Their size and magnetic properties were characterized and analyzed in terms of aggregation and magnetic relaxation, respectively. We analyzed the rheology of these FFs in terms of the shear rate and magnetic field dependence of the viscosity, yield stresses and viscoelasticity, and used the Mn proposed by Vokova [18] and a critical Mason number, $Mn^{*}(\phi)$, to collapse the rheological data for each concentration in a single curve.

3.5 Materials and Methods

3.5.1 Materials

Iron (III) chloride hexahydrate ($FeCl_3 6H_2O$)), cobalt (II) chloride hexahydrate ($CoCl_2$ $6H_2O$), and oleic acid were obtained from Sigma Aldrich. Sodium oleate and 1-octadecene were obtained from TCI America. Ethanol 99.5% anhydrous and acetone were obtained from Fisher Scientific. All materials were used as received. The mineral oil was obtained commercially.

3.5.2 Particle synthesis

Iron oxide and cobalt ferrite nanoparticles were synthesized by thermal decomposition of a metal-oleate precursor. The iron-oxide precursor was prepared by dissolving 6.4 g of $FeCl_3 6H_2O$ and 24.36 g of sodium oleate in a mixture composed of 50 mL ethanol, 50mL distilled water, and 100 mL of hexane. The cobalt ferrite precursor was prepared by dissolving 5.40 g of $FeCl_3 6H_2O$, 2.40 g of $CoCl_2$ $6H_2O$, and 24.36 g of sodium oleate in a mixture composed of 50 mL ethanol, 50 mL distilled water, and 100 mL of hexane. For both syntheses the mixture was magnetically stirred at 70ºC for 4 hrs under reflux. After this, an organic metal oleate complex and an aqueous phase were obtained. The organic phase was separated and washed by adding 30 mL of distilled water in a separation funnel. The resulting mixture was heated in a vacuum oven at 70ºC for 3 days for complete evaporation of the remaining hexane and ethanol.

To synthesize the iron oxide and cobalt ferrite nanoparticles, 0.06M and 0.1 M solutions were prepared by dissolving each metal oleate complex in 1-octadecene with 0.08M oleic acid. The reaction mixture was heated in a 500 mL three neck flask to 320ºC

at 3.3 ºC/min and then kept at that temperature for one and onle-half hours for iron oxide, and three hours for cobalt ferrite, followed by cooling to room temperature. When the reaction had reached room temperature, a mixture of acetone and ethanol was added in a 1:3 proportion to precipitate the magnetic nanoparticles and obtain a waxy material. This material was washed with acetone and chloroform in equal proportions. Afterwards a dry powder-like material was obtained.

3.5.3 Sample preparation

Samples were prepared by weighing specific amounts of the magnetic nanoparticles in a crystal vial, followed by addition of the mineral oil. Manual agitation was performed with a glass rod, followed by sonication for 30 minutes at room temperature. Samples were prepared with magnetic particle loadings between 0.01 and 5 %v/v. Although the objective was to prepare equal volume concentrations of iron oxide and cobalt ferrite particles for comparison purposes, similar concentrations were achieved within the same order of magnitude. Particle precipitation was verified by placing a rare earth magnet on the prepared FF vial. No precipitation was observed throughout the duration of the study (7 months).

3.5.4 Ferrofluid characterization

Transmission electron microscopy (TEM) using a Zeiss Leo 922 TEM was used to study the core size distribution of the magnetic nanoparticles. Carbon coated copper grids were submerged in a suspension of particles in hexane, followed by evaporation of hexane in a vacuum oven. The hydrodynamic size distribution of the particles was measured using a Brookhaven Instruments BI 90-Plus dynamic light scattering (DLS)

instrument. Particles were suspended in hexane and filtered with PTFE filters (0.4μm). Dilute suspenions $\left(\phi_m = 0.0001\right)$ of the iron oxide and cobalt ferrite particles were prepared. These were also used for the study of the size distribution of the particles with application of magnetic fields. This was performed by placing a rare earth magnet on top of the DLS cuvette. The volume weighted hydrodynamic diameters are reported.

The equilibrium and dynamic magnetization response and the AC susceptibility of the ferrofluid were studied using a Quantum Design MPMS-XL7 Superconducting Quantum Interference Device (SQUID) magnetometer. The equilibrium magnetization behavior of ferrofluids was described using the Langevin function and taking into account the particle's lognormal size distribution. Whereas the dynamic magnetization was fitted using the Debye model [27].

Optical microscopy images of the ferrofluids were obtained using an Olympus BX51 polarized microscope equipped with a Canon camera model EOS Rebel. The ferrofluids were sandwiched between two microscope glass slides. Images of the ferrofluids under application of magnetic fields were obtained by placing a rare earth cylindrical magnet in front of the microscope as close as possible to the glass slides. The magnetic field exerted on the ferrofluid was measured by placing a Magnet-Physik FH 54 Gauss-Tesla meter (Hall probe) directly on top of the glass slides.

3.5.5 Magnetorheometry

An Anton Paar Physica MCR-301 series rheometer equipped with a magnetorheological device (MRD) was used for the experiments. The measurements were carried out with a 15 mm diameter cone/plate fixture and a gap of 0.02 mm. Applied magnetic fields were in the range of 10-650 mT. Direct measurement of the magnetic

field near the sample was possible using a Hall probe (Magnet-Physik FH 54 Tesla Gauss meter) located just below the sample plates. Due to heat dissipation by the induction coil used to generate the magnetic fields, temperature had to be controlled using a Julabo water bath connected in a feedback control loop. Direct temperature measurement was possible using a thermocouple located just below the sample plates.

Sample loading was carried out as follows. The sample was loaded onto the stationary lower plate of the rheometer and the upper plate was lowered until the set gap height. The sample was then presheared for 5 minutes at 100 s^{-1}. Afterwards the suspension was left to equilibrate for a period of 5 minutes. The viscosity of each ferrofluid was measured at a constant set temperature of 25^{o}C by applying a logarithmic decreasing shear rate and measuring the steady state viscosity. When applying magnetic fields, a constant field was applied throughout the entire shear rate range studied. Magnetic fields were applied in an increasing manner. Demagnetization of the coil was performed after reaching the highest applied field. This was done to avoid trapped flux (remanecence) in the coils, which would affect the target magnetic field. Oscillatory measurements of the elastic and viscous moduli of the ferrofluids were measured as a function of increasing applied magnetic field at constant oscillatory frequencies ranging from 0.1 to 50 rads/s, and a constant strain of 1%.

3.6 Results and Discussion

3.6.1 Ferrofluid characterization

Figure 1 illustrates the core size distribution of the nanoparticles, which were found to be 17.6±0.38 nm for iron oxide and 9.6±0.05 nm for the cobalt ferrite particles. Equilibrium magnetization curves for the iron oxide and cobalt ferrite ferrofluids used in our experiments are shown in **Figure 2**. Initially, at low applied magnetic fields the fluid's magnetization is linearly dependent on the applied magnetic field, but eventually saturates at high magnetic fields as the particle's magnetic moments become predominantly aligned in the field direction. The saturation magnetization increases with increasing particle concentration. The inset corresponds to the highest particle content. A non-linear fit to the Langevin function resulted in an average magnetic core size of 8 nm for iron oxide and 11 nm for the cobalt ferrite, respectively. The latter had greater polydispersity, as evidenced by the geometric deviation $\left(\ln\phi = 0.2\right)$, compared to the iron oxide particles $\left(\ln\phi = 0.6\right)$. Particle magnetic volume fractions were also obtained from the non-linear fit, and are summarized in **Table 1**. The cobalt ferrite FFs in general had larger particles and slightly higher concentrations.

The Brownian relaxation of the cobalt ferrite particles was verified through AC susceptibility measurements **(Figure 3).** Theoretical calculation of the Brownian relaxation time of the particles, is given by,

$$\tau_B = \frac{3V\eta}{k_B T} \qquad \textbf{(3)}$$

where V is the hydrodynamic volume of the particles, η is the viscosity of the suspension media, k_B is Boltzmann's constant, and T is the absolute temperature. This calculation results in a value of 2.3 milliseconds. Experimental Brownian relaxation of the particles is obtained using the frequency at the peak of the out-of-phase susceptibility of the particles from Debye's model [27] χ'', where $\Omega\tau_B = 1$. It is important to note that this peak shifts to lower frequency values as the particle concentration increases, meaning that dipole-dipole interparticle interactions occur. Calculation of the experimental Brownian relaxation time of each FF is summarized in **Table 1**. The experimental Brownian relaxation time of each FF compared to the theoretical time differs by 9 msecs maximum, this difference due to the increments of interparticle interactions as the particle concentration increases. The lowest two concentrations have the same Brownian relaxation, differing to the theoretical by three milliseconds.

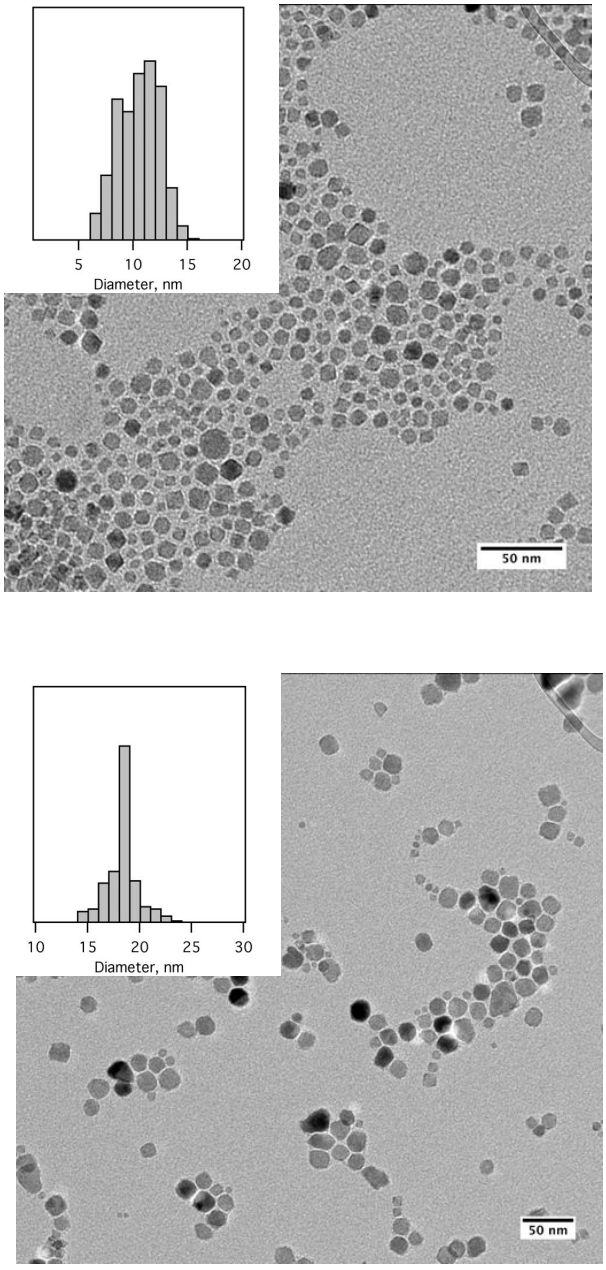

Figure 1. TEM images of the magnetite and cobalt ferrite particles used to prepare the ferrofluids.

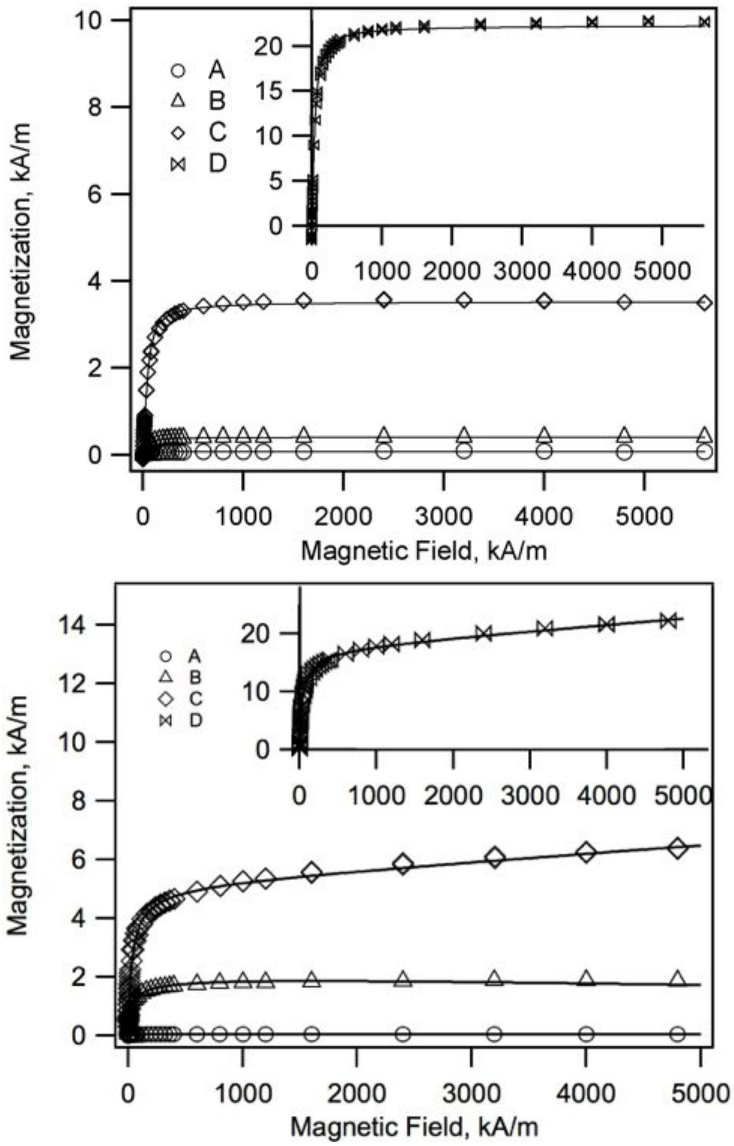

Figure 2. Equilibrium magnetization curves of the prepared ferrofluids of magnetite and cobalt ferrite. Inset corresponds to the most concentrated samples in each set.

Table 1. Magnetic volume fraction of iron oxide and cobalt ferrite particles obtained from a non-linear Lagevin fit, and the Brownian experimental and theoretical relaxation times of the cobalt ferrite ferrofluids.

Sample	Concentration, % v/v		Brownian time	
	Iron Oxide	Cobalt Ferrite	$\tau_{B,\exp}, ms$	$\tau_{B,theory}, ms$
A	0.01	0.02	5.7	2.3
B	0.1	0.4	5.7	
C	0.8	1.1	6.34	
D	5	4	11.7	

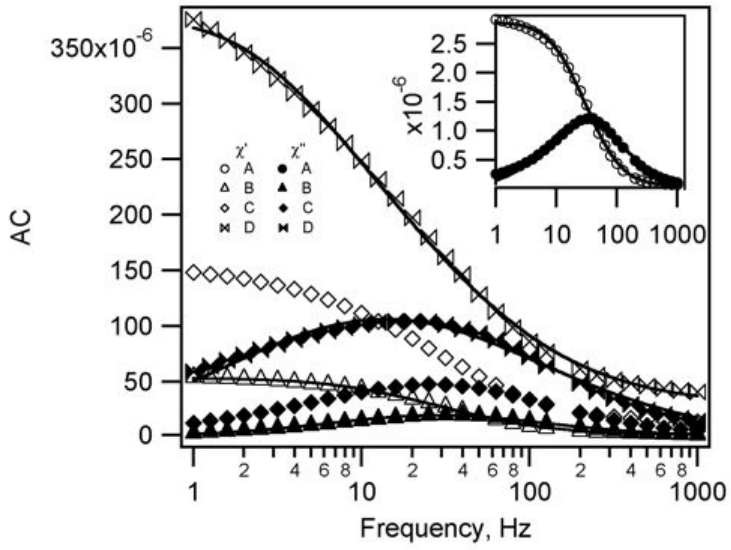

Figure 3. AC Susceptibility curves of the cobalt ferrite based ferrofluids.

Measurements of the hydrodynamic diameter distribution of the particles were performed initially with no magnetic field, resulting in 15.4±0.1 nm for iron oxide and 19±0.1 nm for cobalt ferrite, respectively (Figure 4). Afterwards increasing magnetic fields were applied by placing a rare earth magnet on top of the glass cuvette. This resulted in increasing particle size of up to 516 nm for iron oxide and 1345 nm cobalt ferrite, respectively.

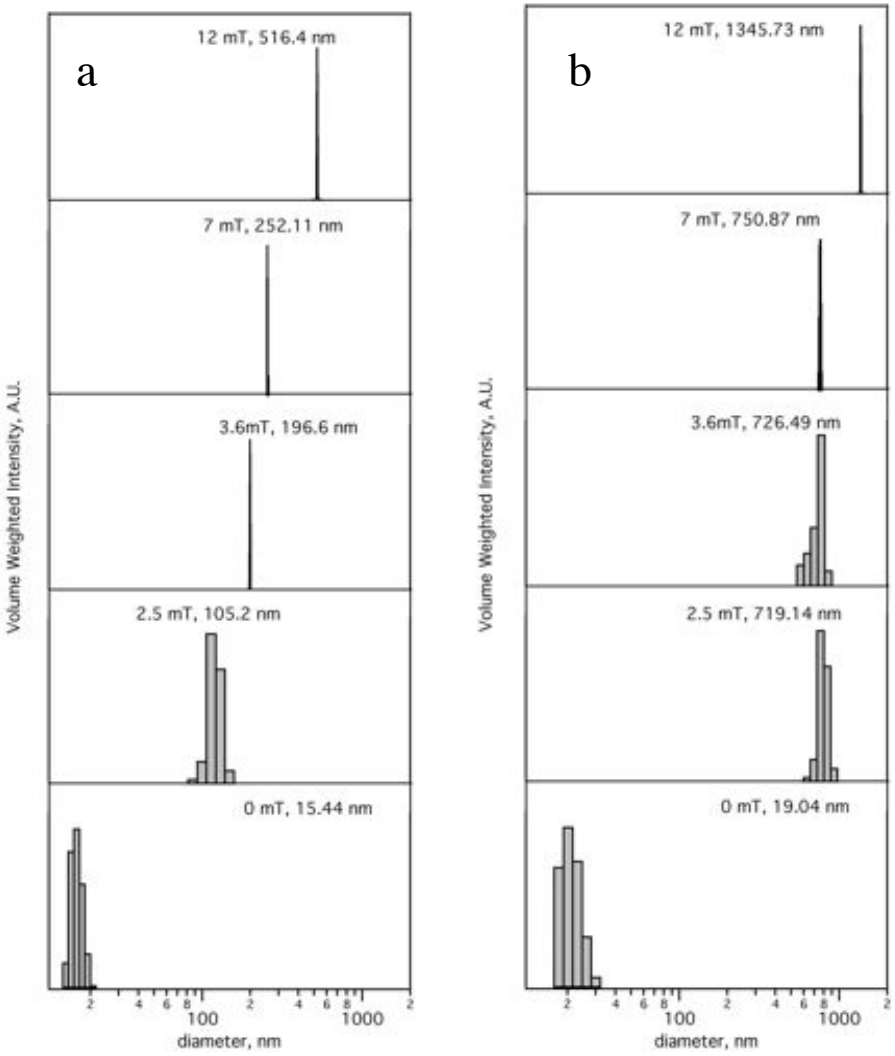

Figure 4. Dynamic light scattering of the iron oxide (a) and cobalt ferrite (b) nanoparticles suspended in hexane with and without the application of external magnetic fields.

Figure 5 shows representative optical microscopy images of the iron oxide and cobalt ferrite ferrofluids with no magnetic field and with applied magnetic field of 21 mT. Initially cobalt ferrite showed some aggregation in the absence of an external magnetic field, not observed in the iron oxide FFs. Also, formation of chain-like aggregates seemed greater in cobalt ferrite FFs, consistent with DLS observations.

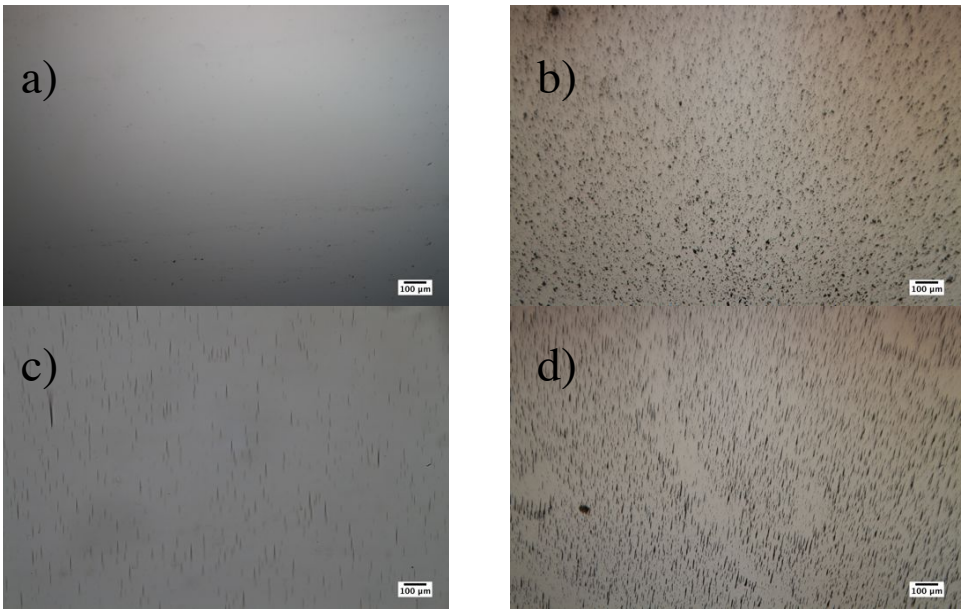

Figure 5. Optical microscopy images of the magnetite (a,c) and cobalt ferrite (b,d) particles (0.1 % v/v) with out the application of an external magnetic field (a,b) and with the application of an external magnetic field of 21 mT (c,d).

3.6.2 Viscosity curves and scaling with Mason number

Figure 6 illustrates the reduced viscosity, defined as the viscosity of FF with an applied magnetic field divided by the viscosity of FF with no magnetic field field at high shear rates, of the iron oxide and cobalt ferrite ferrofluids. At the lowest particle concentration studied (samples (A)), the iron oxide FFs show a measurable shear rate range of almost four decades, while cobalt ferrite was characterized over two decades of

shear rate. At this concentration Newtonian behavior was observed throughout the entire shear rate range studied in both ferrofluids, with increments in viscosity of just 0.01 Pa s, *i.e.*, no dramatic viscosity increase was observed. Increasing particle content by an order of magnitude samples (B) resulted in shear thinning behavior for the iron oxide FF whereas the cobalt ferrite FF did not showed this behavior, even though it was slightly more concentrated. Samples (C) both show shear thinning, although the iron oxide ferrofluids had stronger viscosity response than cobalt ferrite. It is also observed that the cobalt ferrite samples show saturation only at high magnetic fields, whereas the iron oxide FFs saturated at relatively low magnetic fields. Both FFs in sample D show shear thinning behavior with similar viscosity magnitudes and saturation with magnetic field.

Overall, shear thinning is the dominant response for both fluids for intermediate and high concentrations. Increasing particle content (volume fraction) results in an increase in the shear rate range that can be applied and a measurable torque can be obtained. Also, increasing applied magnetic fields leads to a merging of the viscosity curves, i.e. saturation of the magnetic field effect. Greater magnetic field dependence occurs at low shear rates. It is important to mention that both particles reached relatively similar viscosity increases with the highest particle content and applied magnetic fields, even though the cobalt ferrite FFs had slightly higher concentration and larger particles than the iron oxide FFs.

We fitted the viscosity curves shown in Figure 6 to a power law model in the low shear rate region only. The model used was,

$$\eta = c\,\dot{\gamma}^{-n} + \eta_{\infty} \qquad \textbf{(4)}$$

where c, n, and η_∞ are fitting parameters, the latter corresponding to the high shear rate viscosity. This resulted in magnetic field independent slopes ranging from 0.51 to 0.91 for the iron oxide FFs and from 0.62 to 0.95 for the cobalt ferrite FFs.

Figure 7 illustrates the individual scaling of the viscosity curves of Figure 6 using a modified version of equation (1), where relative permeability was used instead of β. Iron oxide samples scale satisfactorily, whereas the cobalt ferrite samples showed some spread, specifically at intermediate applied fields. For the purposes of this work we have assumed $\mu_c = 1$. Three regions are observed for every concentration and for both particle types: (i) power law viscosity behavior with a negative slope, (ii) viscosity independent of Mn, (iii) and a curved region between region (i) and (ii). **Figure 7** also illustrates fits to,

$$\eta/\eta_\infty = 1 + Mn^*(\phi) Mn^\Delta , \qquad \textbf{(5)}$$

where $Mn^*(\phi)$ was obtained with the intersection of the linear behavior of the η/η_∞ vs shear rate curve with the high shear rate line. This $Mn^*(\phi)$ in our experiments increased with particle concentration, consistent with the work of others [21]. By fitting each sample with Equation 5 results in a magnetic field independent Δ with values ranging from 0.7 to 0.8 for both iron oxide and cobalt ferrite., similar to reports by other authors for inverse FFs [17, 18, 20, 21] **(Table 3)**.

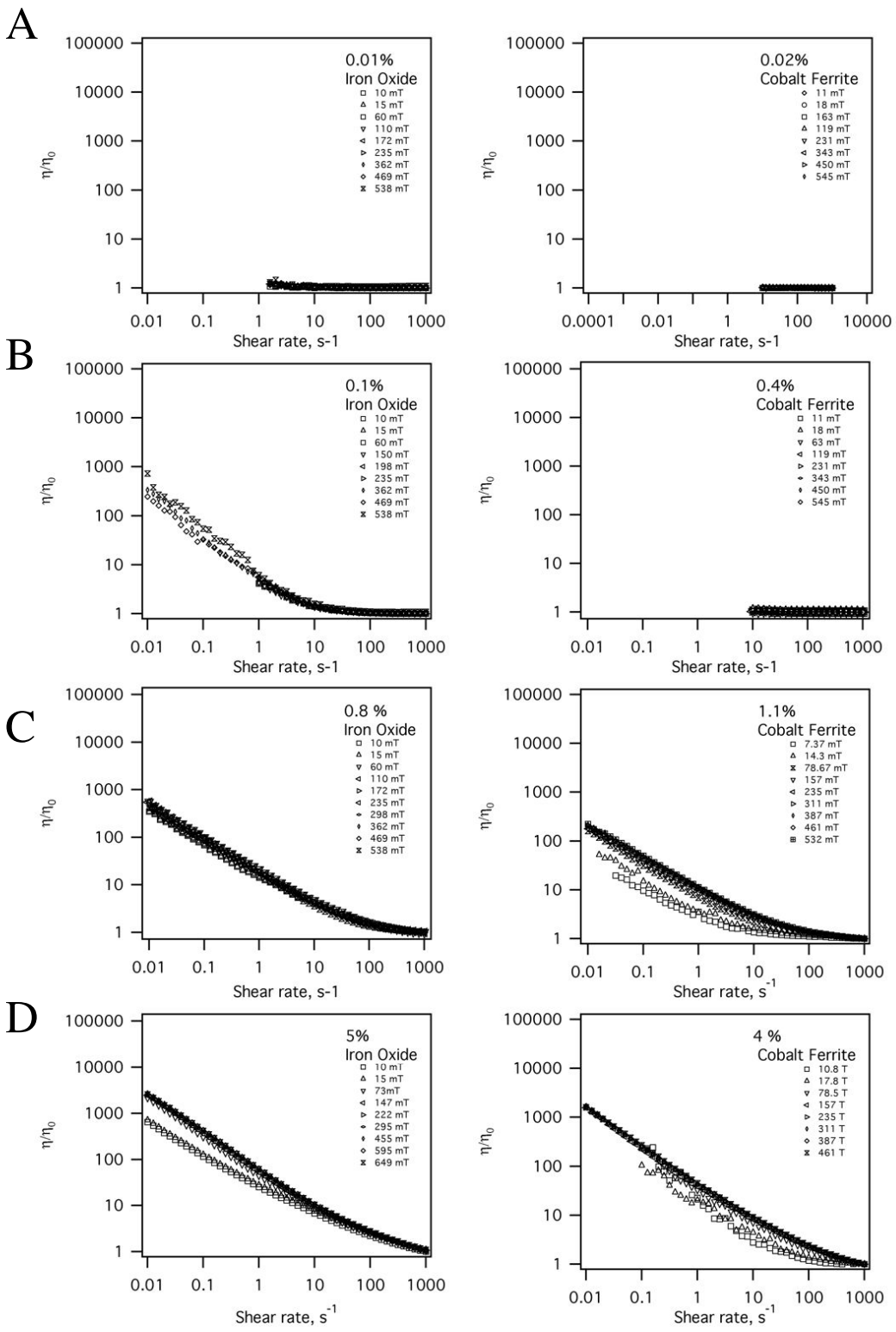

Figure 6. Reduced steady state viscosity of the iron oxide and cobalt ferrite ferrofluids.

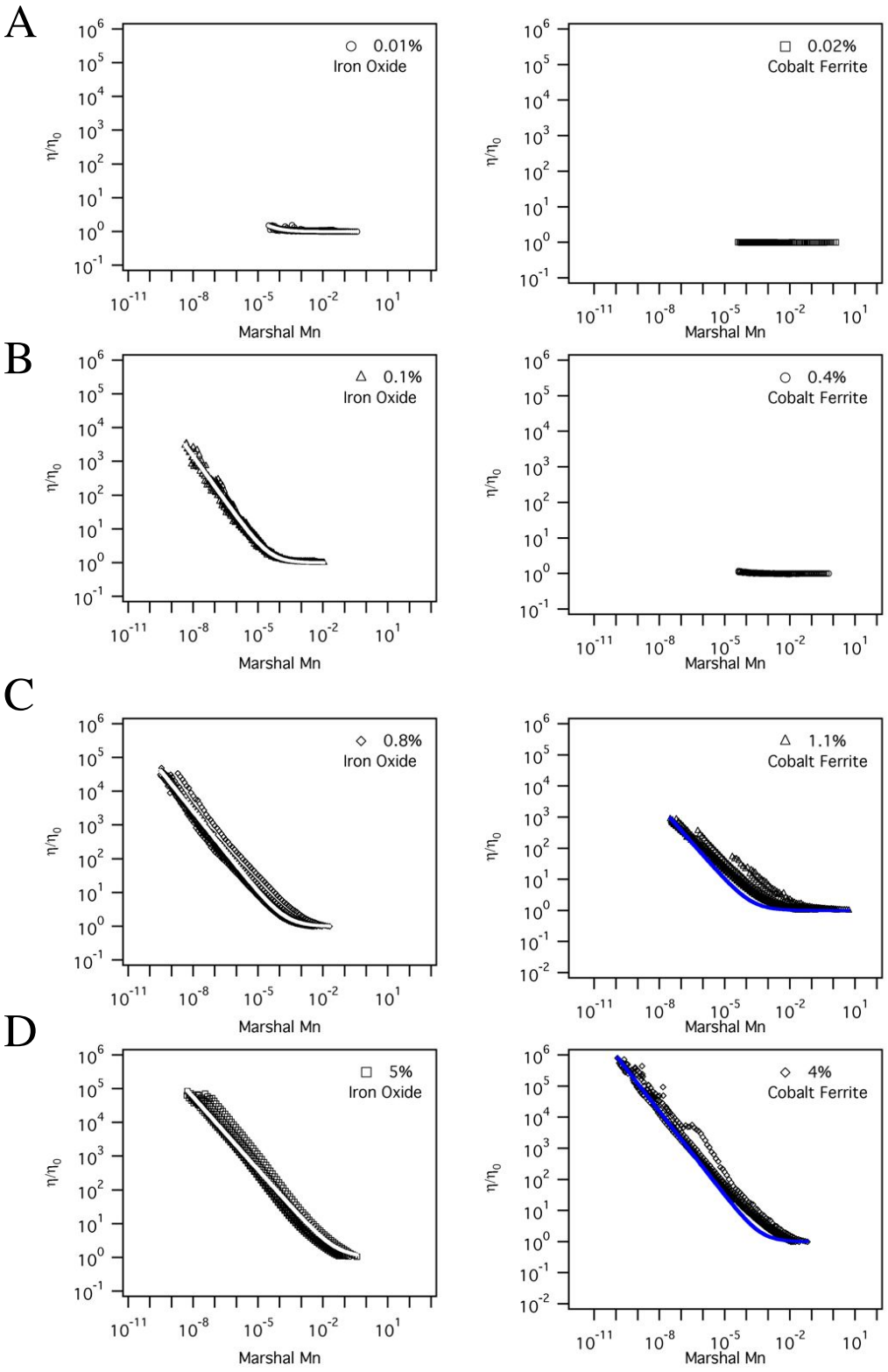

Figure 7. Reduced viscosity as a function of the Mason number for magnetite and cobalt ferrite. Line corresponds to the fit Equation 5 with varying *Mn** determined for each concentration.

Table 1. Fitting parameters for equation 3 fitted to data of **Figure 7**.

	Sample	$Mn^*(\phi)$	**Δ**
Iron Oxide	A	10^{-4}	-0.81±0.004
	B	10^{-4}	-0.89±0.001
	C	10^{-3}	-0.80±0.001
	D	10^{-1}	-0.71±0.001
Cobalt Ferrite	A	-	-
	B	-	-
	C	10^{-3}	-0.79±0.001
	D	10^{-3}	-0.89±0.001

Using $Mn^*(\phi)$ we have collapsed every concentration studied in a single graph by scaling the Mason number as suggested by Marshall *et.al*. [21]. The values used for $Mn^*(\phi)$ are shown in **Table 3**. **Figure 8** shows that plotting reduced viscosity as a function of $Mn/Mn^*(\phi)$ satisfactorily collapses the data for the iron oxide ferrofluids. However, the data for the cobalt ferrite ferrofluids did not collapse when plotted as a function of $Mn/Mn^*(\phi)$. The iron oxide master curve showed a slope of -0.9, close to that predicted by Marshall *et.al*. [21] on the basis of the Bingham model, whereas the cobalt ferrite curves showed varying slopes of 0.66±0.008 to 0.94±0.001.

The shear thinning in both FFs had different slopes. We suspect this difference could be due to the different relaxation mechanisms of the particles in the ferrofluids, and how this couples with an external shearing. In the absence of shear, FFs under the application of magnetic fields form chain-like structures with dipoles aligned head to tail. In the case of iron oxide particles (Neél relaxation) these chains when sheared align at an angle with respect to the applied field due to the balance between magnetic and hydrodynamic torques only on the chain. Although individual particles physically rotate due to the local vorticity, the dipoles remain somewhat aligned head to tail. In the case of

particles with Brownian relaxation, the local vorticity tends to bring the individual particle dipoles out of the favorable head-to-tail alignment, resulting in unfavorable magnetic interactions and break-up of chains. Breakage of chain-like structures of particles that relax by the Neél mechanism occurs due to a balance between hydrodynamic forces pushing particles apart and magnetic particle-particle attractions pulling them together into the chains. On the other hand, when the particles relax by the Brownian mechanism their dipoles are fixed to the crystal structure and must therefore rotate with the particles. As the shear rate increases, the hydrodynamic torque increases to drive the particle dipoles out of head-to-tail alignment, resulting in unfavorable magnetic interactions and therefore break-up of chain-like structures. This rotation, coupled with the magnetic and hydrodynamic forces on the chains, could lead to a different dependence of viscosity on shear rate and magnetic field.

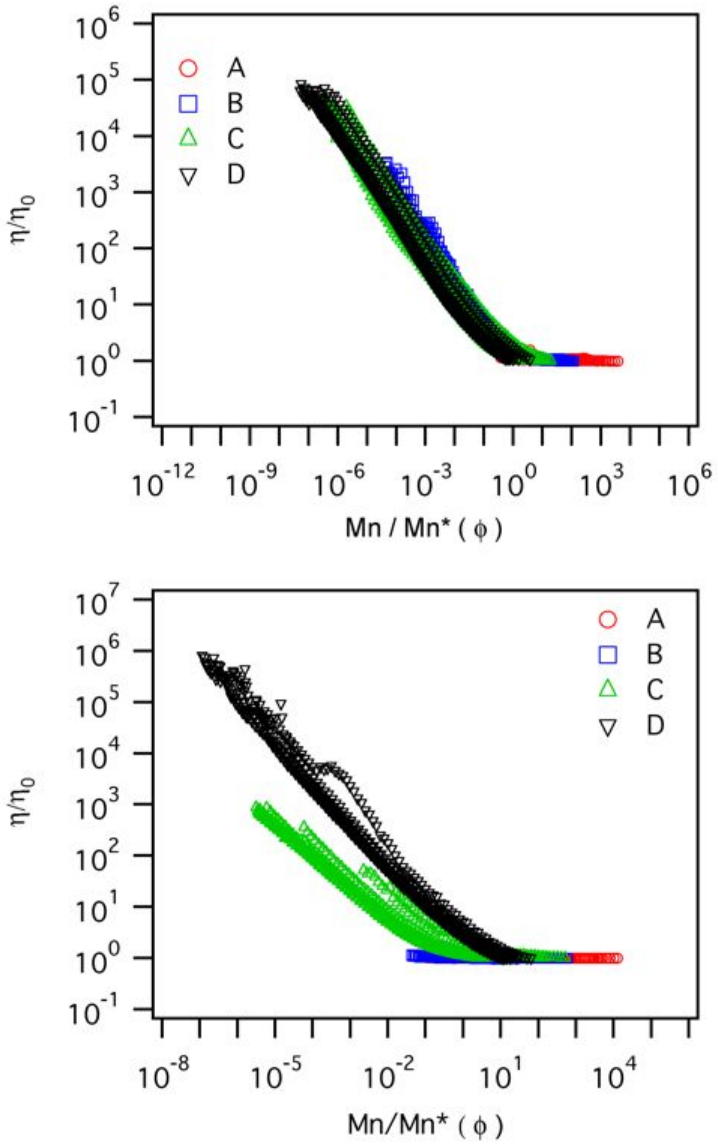

Figure 8. Reduced viscosity as a function of a scaled Mason number, $Mn/Mn^{*}(\phi)$.

3.6.3 Yield stresses and viscoelastic behavior

The iron oxide and cobalt ferrite ferrofluids showed significant yielding behavior, as illustrated in **Figure 9**. The yield stress was determined by fitting the Bingham equation to the experimental stress vs shear rate curves:

$$\tau = \tau_B + \eta_P \dot{\gamma} \quad \textbf{(6)}$$

where τ is the measured stress, τ_B is the resulting yield stress, η_P is the plastic viscosity, and $\dot{\gamma}$ is the shear rate. Increasing the applied magnetic field caused the Bingham yield stress to increase until saturation occurred, where the yield stresses become independent of the applied field in both iron oxide and cobalt ferrite samples. The iron oxide based ferrofluids showed the highest Bingham yield stresses at high particle concentration, however at low particle concentrations cobalt ferrite showed higher yield stresses. These stresses are much higher than other reported values for commercially available ferrofluids [13], where much lower viscosity solvents were used (~60-170 mPa s).

Magnetic field dependent moduli of the iron oxide and cobalt ferrite based ferrofluids measured with increasing constant oscillation frequencies are illustrated in **Figure 10**. Samples (A) of both iron oxide and cobalt ferrite ferrofluids, and sample (B) of cobalt ferrite did not show measurable viscoelastic moduli within the instrument detection limit. The elastic modulus dominates the oscillatory response of both ferrofluids, increasing in intensity with increasing magnetic fields. We believe this elasticity is due to the magnetic interactions between particles in a chain-like arrangement. However, the cobalt ferrite ferrofluids where the only to show a crossover of the elastic and storage modulus at a specific magnetic field, transitioning from viscous to elastic behavior only at a particle concentration of 1 % v/v. Saturation of the moduli

with magnetic fields was not observed within the magnetic field range studied. The moduli of the iron oxide samples became magnetic field independent above applied frequencies of 20 Hz, except at the highest concentration studied (5 % v/v). This sample did not show magnetic field and oscillatory frequency dependent moduli within the magnetic field and oscillatory frequency ranges studied. The iron oxide ferrofluids showed higher measured moduli than the cobalt ferrite samples, under similar conditions. Experimental dynamic shear measurements in ferrofluids have not been reported, however reports for inverse FFs do show an elastic response as a function of magnetic field reaching a plateau at high magnetic fields of approximately 10^3 kA/m [28].

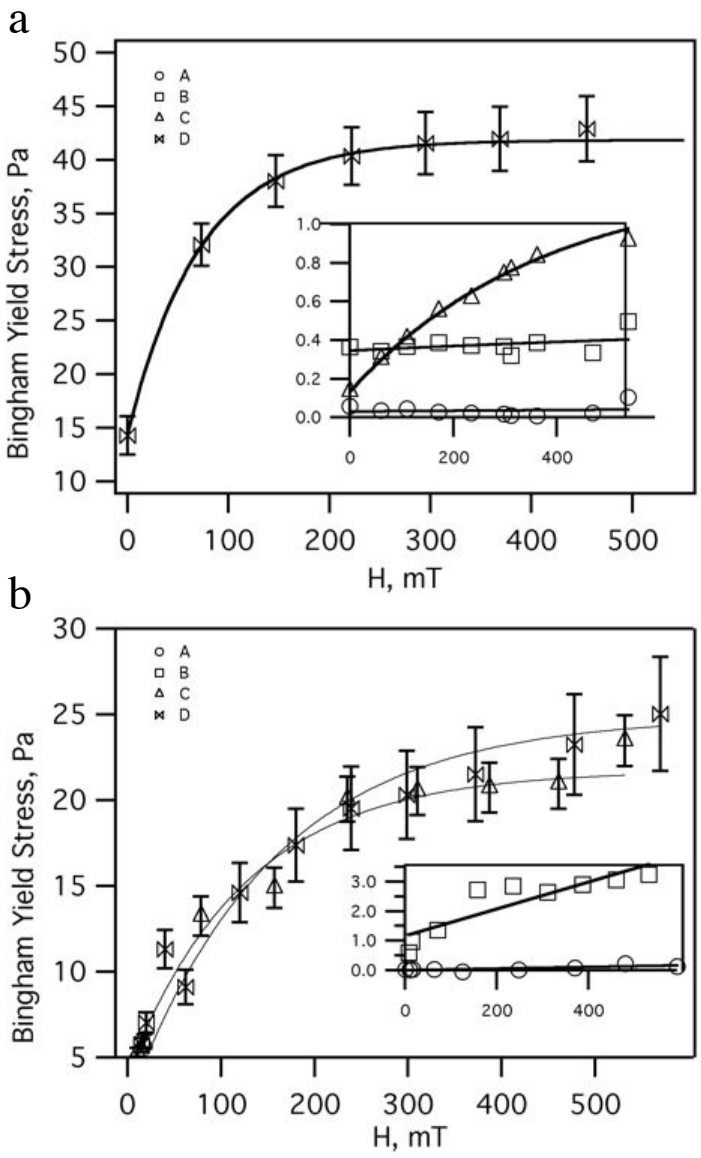

Figure 9. Bingham yield stress for the iron oxide (a) and cobalt ferrite (b) ferrofluids.

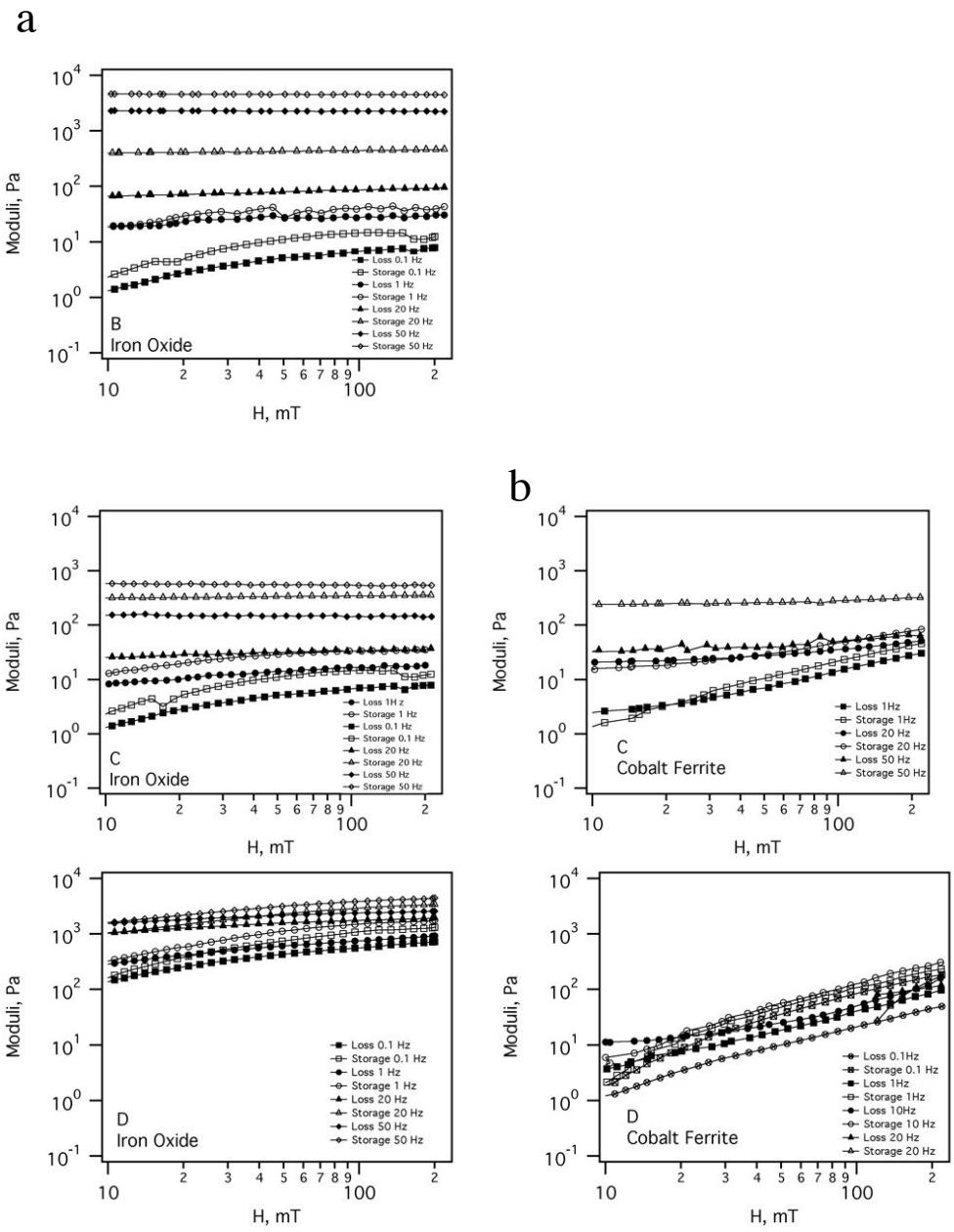

Figure 10. Loss and storage moduli of the iron oxide (a) and cobalt ferrite (b) ferrofluids.

3.7 Conclusion

We synthesized and characterized iron oxide and cobalt ferrite based ferrofluids with particle concentrations ranging from 0.01% to 5% v/v, AC susceptibility measurements showed the cobalt ferrite based ferrofluid had Brownian relaxation while the iron oxide ferrofluid had Neél relaxation. We characterized their rheological properties with the application of magnetic fields ranging from 10 mT to 600 mT. This resulted in viscosity increase of over three decades with decreasing shear rates, following a power law. Both samples showed magnetic field independent slopes, ranging from 0.5 to 0.9. Scaling of the flow curves individually with a Mason number resulted in good agreement for the iron oxide samples, showing a high shear rate plateau followed by linear viscosity increase with decreasing shear rate. The cobalt ferrite ferrofluid showed some spread of the curves although with similar plateau/power law behavior. Collapse of all the viscosity curves was attempted using a scaled Mn defined as $Mn/Mn^{*}(\phi)$, where $Mn^{*}(\phi)$ incorporates the particle concentration effect on the magnetorheology of the ferrofluids. It was shown that iron oxide ferrofluids scaled better with the Mn than cobalt ferrite ferrofluids.

Both ferrofluids showed a measurable Bingham yield stress when magnetic fields where applied, resulting in yield stresses of up to 40 Pa for iron oxide ferrofluids, whereas cobalt ferrite ferrofluids showed yield stresses of up to 25 Pa. Both samples also showed a magnetic field dependent viscoelastic moduli, where the elastic modulus dominated the oscillatory response of the material within the entire magnetic field range studied.

3.8 References

1. Odenbach, S., *Magnetoviscous Effects in Ferrofluids*. 2002, Berlin: Springer.
2. Odenbach, S., *Ferrofluids, Magnetically Controllable Fluids and Their Applications*. 1 ed. 2002, Berlin: Springer.
3. Odenbach, S., *Ferrofluids - magnetically controlled suspensions*. Colloids and Surfaces a-Physicochemical and Engineering Aspects, 2003. **217**(1-3): p. 171-178.
4. Odenbach, S. and H. Stork, *Shear dependence of field-induced contributions to the viscosity of magnetic fluids at low shear rates*. Journal of Magnetism and Magnetic Materials, 1998. **183**: p. 188-194.
5. Pop, L., et al., *Microstructure and rheology of ferrofluids*. Journal of Magnetism an Magnetic Materials, 2005. **289**: p. 303-306.
6. Pop, L.M., et al., *The microstructure of ferrofluids and their rheological properties*. Applied Organometallic Chemistry, 2004. **18**(10): p. 523-528.
7. Pop, L.M. and S. Odenbach, *Investigation of the microscopic reason for the magnetoviscous effect in ferrofluids studied by small angle neutron scattering*. Journal of Physics-Condensed Matter, 2006. **18**(38): p. S2785-S2802.
8. Viota, J.L., J.D.G. Duran, and A.V. Delgado, *Study of the magnetorheology of aqueous suspensions of extremely bimodal magnetite particles*. European Physical Journal E, 2009. **29**(1): p. 87-94.
9. Hong, R.Y., et al., *Rheological properties of water-based Fe3O4 ferrofluids*. Chemical Engineering Science, 2007. **62**(21): p. 5912-5924.

10. Brenner, H. and M. Weissman, *Rheology of a Dilute Suspension of Dipolar Spherical Particles in an External Field. II. Effects of Rotary Brownian Motion*. Journal of Colloid and Interface Science, 1972. **41**(3): p. 499-531.

11. Odenbach, S., T. Rylewicz, and M. Heyen, *A rheometer dedicated for the investigation of viscoelastic effects in commercial magnetic fluids*. Journal of Magnetism and Magnetic Materials, 1999. **201**: p. 155-158.

12. Ghasemi, E., A. Mirhabibi, and M. Edrissi, *Synthesis and rheological properties of an iron oxide ferrofluid*. Journal of Magnetism and Magnetic Materials, 2008. **320**(21): p. 2635-2639.

13. Shahnazian, H. and S. Odenbach, *Yield stress in ferrofluids?* International Journal of Modern Physics B, 2007. **21**(28-29): p. 4806-4812.

14. Soto-Aquino, D., D. Rosso, and C. Rinaldi, *Oscillatory shear response of dilute ferrofluids: Predictions from rotational Brownian dynamics simulations and ferrohydrodynamics modeling*. Physical Review E, 2011. **84**(5).

15. Martin, J.E. and R.A. Anderson, *Chain model of electrorheology*. Journal of Chemical Physics, 1996. **104**(12): p. 4814-4827.

16. Halsey, T.C., J.E. Martin, and D. Adolf, *Rheology of electrorheological fluids*. Physical Review Letters, 1992. **68**(10): p. 1519-1522.

17. de Gans, B.J., et al., *Linear viscoelasticity of an inverse ferrofluid*. Physical Review E, 1999. **60**(4): p. 4518-4527.

18. Volkova, O., et al., *Magnetorheology of magnetic holes compared to magnetic particles*. Journal of Rheology, 2000. **44**(1): p. 91-104.

19. Zubarev, A.Y. and L.Y. Iskakova, *On the theory of rheological properties of magnetic suspensions*. Physica a-Statistical Mechanics and Its Applications, 2007. **382**(2): p. 378-388.

20. Ramos, J., et al., *Steady shear magnetorheology of inverse ferrofluids*. Journal of Rheology, 2011. **55**(1): p. 127-152.

21. Marshall, L., C.F. Zukoski, and J.W. Goodwin, *EFFECTS OF ELECTRIC-FIELDS ON THE RHEOLOGY OF NON-AQUEOUS CONCENTRATED SUSPENSIONS*. Journal of the Chemical Society-Faraday Transactions I, 1989. **85**: p. 2785-2795.

22. Klingenberg, D., J. Ulicny, and M. Golden, *Mason number for magneorheology*. Journal of Rheology, 2007. **51**(5): p. 883-893.

23. Melle, S., et al., *Microstructure evolution in magnetorheological suspensions governed by Mason number*. Physical Review E, 2003. **68**(4): p. 11.

24. de Gans, B.J., H. Hoekstra, and J. Mellema, *Non-linear magnetorheological behaviour of an inverse ferrofluid*. Faraday Discussions, 1999. **112**: p. 209-224.

25. Kroell, M., et al., *Magnetic and rheological characterization of novel ferrofluids*. Journal of Magnetism an Magnetic Materials, 2005. **289**: p. 21-24.

26. Zubarev, A.Y., J. Fleischer, and S. Odenbach, *Towards a theory of dynamical properties of polydisperse magnetic fluids: Effect of chain-like aggregates*. Physica a-Statistical Mechanics and Its Applications, 2005. **358**(2-4): p. 475-491.

27. Fannin, P.C., B.K.P. Scaife, and S.W. Charles, *The Measurement of the Frequency-dependent Susceptibility of Magnetic Colloids*. Journal of Magnetism and Magnetic Materials, 1988. **72**(1): p. 95-108.

28. Ramos, J., J. de Vicente, and R. Hidalgo-Alvarez, *Small-Amplitude Oscillatory Shear Magnetorheology of Inverse Ferrofluids*. Langmuir. **26**(12): p. 9334-9341.

4 A Comparison of the Magnetorheology of Two Ferrofluids with Different Magnetic Field Dependent Aggregation Behavior.

4.1 Abstract

The effect of magnetic field induced particle aggregation on the magnetorheology of commercial iron oxide based ferrofluids was investigated by means of comparison of a ferrofluid with particles that resist aggregation and a ferrofluid with particles that interact when a field is applied, forming chain-like aggregates. This difference between the two ferrofluids was confirmed by optical microscopy and dynamic light scattering (DLS) measurements in an applied magnetic field. Both fluids had similar magnetic particle fraction, but showed very different magnetorheological behavior. Aggregation resulted in a stronger magnetic field dependent viscosity enhancement, and the appearance of an elastic modulus. The latter was not observed in the non-aggregated ferrofluid. The magnetorheology of these two fluids was described using the Mason number, resulting in two distinct Mn power law slopes at intermediate and small Mn values for the ferrofluid with magnetic field induced aggregation.

4.2 List of Figures

4.3 Introduction

Ferrofluids (FFs) are colloidally stable dispersions of single domain magnetic nanoparticles undergoing rotational and translational Brownian motion in a non-magnetic liquid carrier. The particles are typically magnetite (Fe_2O_3) or cobalt ferrite ($CoFe_2O_4$), range from 5-15 nm in diameter, and are suspended at concentrations of up to 10% v/v. Solvents used for preparing ferrofluids are usually oils, organic solvents and water.

Particle interactions in FFs include van der Waals attraction, steric/electrostatic repulsions, and magnetic dipole-dipole interactions. The latter are commonly estimated using the interaction parameter λ [1], given by,

$$\lambda = \frac{\mu_0 \, m_s^2 \, V^2}{24 \, k_B \, T} \tag{1}$$

where μ_0 is the permeability of free space, m is the magnetic moment, V is the volume of the particles, k_B is Boltzman constant and T is the temperature. This parameter is commonly used to predict interactions between magnetic nanoparticles through a balance of magnetic and thermal energies [2-5]. DeGennes and Pincus [6] predicted the existence of chains of particles in a FF due to attractive/repulsive dipolar interactions at a threshold value of $\lambda \sim 3$, causing a marked increase in the particle interactions as a result of the dipolar energy exceeding the thermal energy, resulting in chain formation in the equilibrium state. Zubarev and co-workers [7] developed a chain formation model for weakly-interacting fluids $(\lambda << 1)$. Ivanov and co-workers [5] considered strong particle interactions $(\lambda >> 1)$ in the chain formation model of Zubarev *et.al.*, predicting larger particle aggregates compared to a weakly interacting fluid. Stronger interactions resulted

in a marked increase in chain formation, with saturation in chain length with increasing magnetic field. Other authors have used the interaction parameter λ in simulations to study magnetic behavior of aggregated structures using Monte Carlo simulations [8], mean-field Focker-Planck equation [9], and molecular dynamics [10], all of them resulting in an increase of chain length with increasing λ.

Experimental studies with magnetic fluids seem to be in agreement with reported simulations. Typically magnetite particles ranging in 5-10 nm in diameter show interactions to a certain degree using scattering techniques [11, 12]. However dipolar interactions with particles of this size are small and therefore one has to increase experimentally other variables such as the bulk magnetization of the particles. Cobalt [13, 14] and iron [15, 16] nanocrystals have been synthesized with $\lambda \sim 2.5$, and even $\lambda \sim 7$ [17] having larger bulk saturation magnetization. Cryo-TEM images of magnetite with a diameter of approximately 20 nm $(\lambda \sim 7)$ show chains of particles, in contrast to smaller particles of approximately 16 nm $(\lambda \sim 2)$ where the interaction is dominated by repulsive interactions and no chains are observed [17].

Since FFs are magnetic field responsive fluids, they show changes in their properties upon exposure to magnetic fields. These types of fluids have attracted great interest due to their magnetic field dependent reversible flow properties such as viscosity increase, visco-elastic behavior, and induced yield stresses. Application of external fields leads to a magnetic field dependent viscosity enhancement, marked by the appearance of shear thinning behavior. In FFs this is commonly referred to as the "magnetoviscous effect" [3]. Odenbach and co-workers [3, 18-21] have experimentally studied viscosity changes for various commercial concentrated magnetite-based ferrofluids of 20-40%

magnetic particle volume fraction with shear rates between 0-100 s^{-1} and magnetic fields of 50-160 kA/m using a custom made rheometer with a cone-and-plate fixture. Additionally, they also reported yield stresses in magnetite and cobalt ferrite based ferrofluids of 0.05 and 0.07 Pa with applied fields of 30 and 80 kA/m [22]. Recently, Hong and Ghasemi reported the magnetoviscous effect in magnetite based ferrofluids, showing viscosity changes of almost two orders of magnitude with magnetic fields using a wider shear rate range [23, 24]. Yield stresses and viscosity increases in magnetic field responsive fluids are a consequence of the magnetic interactions between particles which leads to the formation of chain-like structures upon application of magnetic fields.

Due to the potential applications of magnetic field responsive fluids [25-27], there is ongoing research towards tuning their properties such as yield stress and viscosity enhancement. It has been demonstrated that enhancement of yield stress of magnetorheological fluids can be achieved with bidisperse particles [28, 29], magnetic fibers [29] and by adding non-magnetic particles [30]. For FFs, an enhanced magnetoviscous effect has been obtained by adding weak dipolar interactions to moderately concentrated FFs, through formation of loose chain-like aggregates [9]. Others suggest replacing the nanoparticles with nanorods, and using polydisperse particles [31].

Our work focuses on comparing experimentally the magnetic properties and the magnetorheology of two ferrofluids with a magnetic field dependent aggregation behavior to show that tunning of stabilization of particles leads to an induced aggregation and stronger magnetoviscous effect, even though the calculated interaction parameters are similar. We will show that poorly stabilized particles display magnetic field

dependent chaining behavior (large particle interactions) even though calculation of the interaction parameter predicts otherwise $(\lambda << 1)$. We studied the magnetorheology of these two fluids and illustrate how interactions affect these properties.

4.4 Materials and Methods

4.4.1 Commercial Ferrofluids

The ferrofluids used for these experiments and the stock dilution fluid were generously provided by FerroTec. Samples were used as received and stored at ambient temperature. Two kinds of samples were received, one with well stabilized particles (FF-A) and another with poorly stabilized particles (FF-B). Neither ferrofluid showed signs of particle precipitation during storage or during any of the experiments reported here, over a period of 6 months.

4.4.2 Characterization of Ferrofluids

The particle hydrodynamic diameters were measured using a Brookhaven Instruments BI 90-Plus Dynamic Light Scattering (DLS) particle size analyzer. We report the volume weighted hydrodynamic diameter distributions. The suspensions were measured in a glass cuvette by first filtering the samples with a glass syringe and Teflon filter (PTFE 0.4 μm). Measurements of the change in hydrodynamic diameter under the application of an external magnetic field were done by placing a rare earth cylindrical permanent magnet on top of the glass cuvette of the DLS while measuring the size of the particles. The core size of the magnetic particles was measured using a Carl Zeiss Leo 922 Transmission Electron Microscope (TEM) operated at 200keV. Particles were suspended in *n*-hexane and deposited in carbon coated copper grids.

Optical microscopy images of the ferrofluids were obtained using an Olympus BX51 polarized microscope equipped with a Canon camera model EOS Rebel. The as-received ferrofluids were sandwiched between two microscope glass slides. Images of the ferrofluids under application of magnetic fields were obtained by placing a rare earth cylindrical magnet in front of the microscope as close as possible to the ferrofluids. The magnetic field exerted on the ferrofluid was measured by placing a Magnet-Physik FH 54 Gauss-Tesla meter (Hall probe) directly on top of the glass slides.

The magnetic behavior of the ferrofluids was studied using a Quantum Design MPMS XL-7 Superconducting Quantum Interference Device (SQUID) magnetometer. Magnetization curves were measured at a fixed temperature of 300 K and fitted using nonlinear regression to the Langevin model weighted by the lognormal size distribution [32].

Rheological measurements of the samples were performed using an Anton Paar Physica MCR 301 series rheometer with a Magnetorheological Device (MRD). This device applies magnetic fields normal to the applied shear deformation using a 15 mm cone and plate fixture with a 0.02 mm gap. With this attachment a current is fixed by the user and the magnetic field is generated by a coil. A Magnet-Physik FH 54 Gauss-Tesla meter positioned below the stationary lower plate allows for measurement of the actual magnetic field at the sample while measuring the rheological properties. Additionally, the sample temperature was measured using a thermocouple, also placed below the lower plate, and controlled through a feedback loop using a Julabo F-25 water/ethanol bath. Sample loading was performed in the following manner. The sample was loaded onto the lower stationary plate of the rheometer followed by lowering the upper plate. After this, a

pre-shear at 100 s^{-1} for 5 minutes was applied and the sample was left to relax for 5 minutes before any measurements. Additionally, demagnetization of the MRD coil and the sample was performed after every measurement. This was done to avoid trapped flux (remanecence) in the coils which would affect the target magnetic field.

Steady state viscosity curves were measured by applying a constant shear rate and measuring the viscosity until steady state was achieved at each shear rate. This was repeated by decreasing the shear rate until the lower end of the detectable torque range of the instrument (10^{-9} N m) was reached. A constant magnetic field was applied for each curve. A similar procedure was used for steady state viscosity measurements as a function of the applied magnetic field, where constant shear rates were applied for each curve. Oscillatory measurements of the elastic and viscous moduli of the ferrofluids were measured as a function of applied external magnetic field at constant oscillatory frequencies of 1, 10, and 50 rads/s, and a strain of 1%.

4.5 Results and Discussion

4.5.1 Physical and Magnetic Characterization of the Ferrofluids

TEM images show particles of similar size in both ferrofluids (**Figure 1**). Fitting the measured sizes to a log-normal distribution resulted in diameters of 11.9 $\pm$ 0.1 nm and 13.9 $\pm$ 0.2 nm, for FF-A and FF-B respectively. The hydrodynamic size distributions of both ferrofluids are illustrated in **Figure 2**, with and without an applied magnetic field. For this measurement the ferrofluids were diluted with their solvent (the suspending medium provided by Ferrotec) to a volumetric particle fraction of 0.0003 (confirmed by SQUID measurements of the saturation magnetization) to allow for DLS measurements which require translucent solutions. In the absence of an applied magnetic field, FF-A and FF-B show a hydrodynamic size of 18.4 nm and 18.1 nm, respectively. Application of an external magnetic field of approximately 79.9 kA/m to both samples resulted in an increase in size from 18.1 nm to 701.8 nm for FF-B (not well stabilized FF), whereas the hydrodynamic size of FF-A (stabilized FF) remained constant.

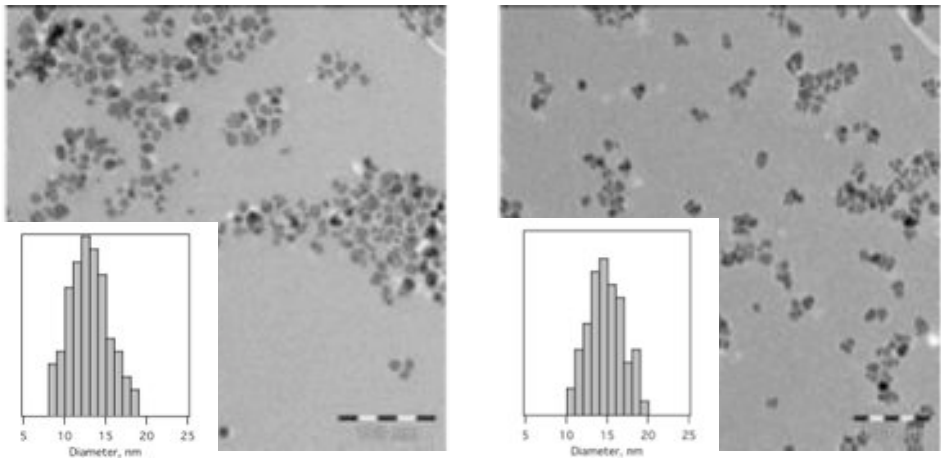

Figure 1. Transmission electron microscopy of FF-A (left) and FF-B (right). The figure inset corresponds to the size distribution of the particles in the images, scale bar corresponds to 100 nm.

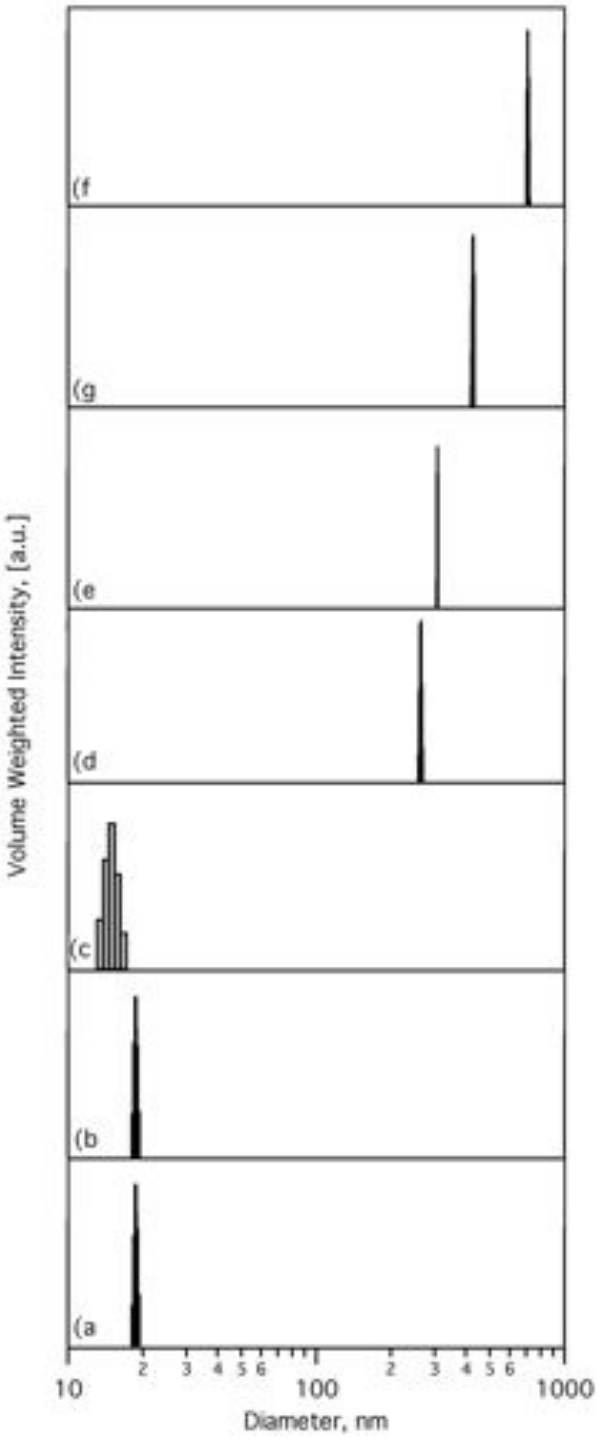

Figure 2. Hydrodynamic size distributions of samples FF-A and FF-B with and without an applied external magnetic field measured by DLS. a) and c) are FF-A and FF-B with no applied external magnetic field, b) is FF-A with a field of 9.5 kA/m, d), e), f), and g), correspond to FF-B with an external applied field of 0.08 kA/m, 1.9 kA/m, 2.8 kA/m, and 9.5 kA/m respectively.

Optical microscopy images of the magnetic nanoparticles are shown in Figure 3. The top images correspond to zero magnetic field, whereas the bottom images correspond to an applied field of 16 kA/m. Application of a field of 16 kA/m induces chain formation in FF-B, with chains of approximately 100 μm in length. FF-A showed some chains of particles with similar length, although in much less quantity.

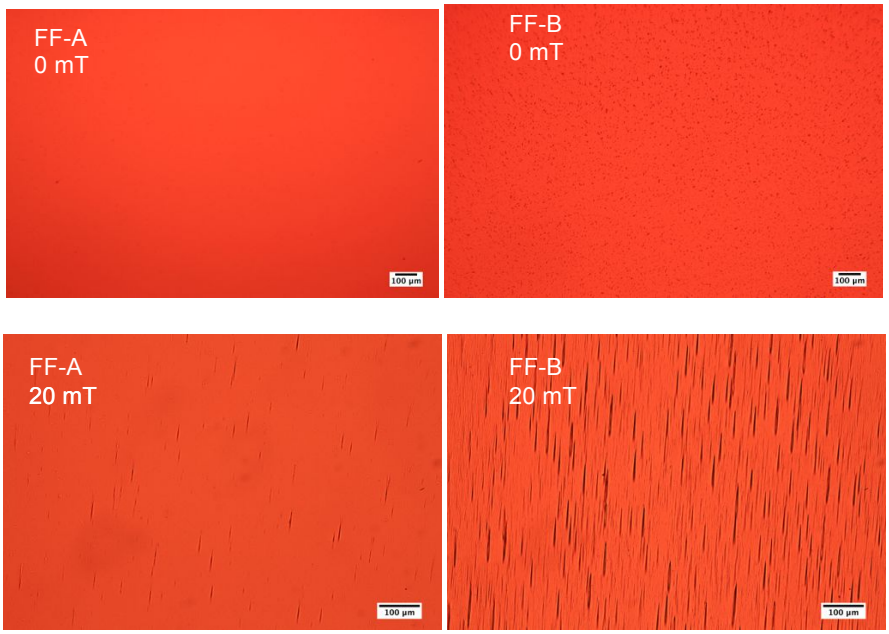

Figure 3. Optical microscopy images of the ferrofluids FF-A and FF-B with no applied magnetic field (top) and with a field of 20 mT (bottom).

Magnetization curves for FF-A and FF-B are shown in Figure 4, where markers correspond to the experimental data, while the solid line corresponds to a nonlinear fit to the Langevin function weighted by the lognormal size distribution. From the non-linear fit to the Langevin function the magnetic particle volume fraction ϕ was 8% v/v for FF-A and 7% v/v for FF-B, whereas the magnetic core diameter was 10.7 nm for FF-A and 11.7 nm for FF-B. Thus, both fluids had similar magnetic properties.

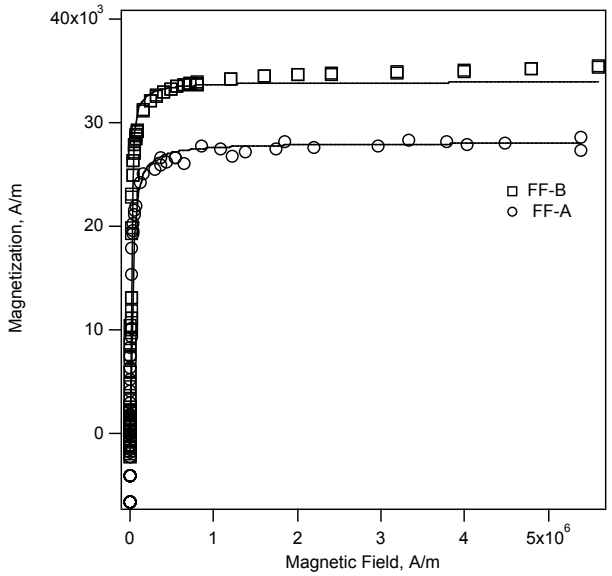

Figure 4. Equilibrium magnetization behavior of FF-A and FF-B.

We have calculated the interaction parameter (λ) for both FF-A and FF-B ferrofluid with the experimentally obtained magnetic core diameter, resulting in 1.3 for FF-A and 1.7 for FF-B. Interestingly, for both FF-A and FF-B, no significant particle chain formation should be expected according to this parameter since $\lambda \approx 1$, the threshold of magnetic energies dominating the thermal energies has not been reached. Results from DLS and optical microscopy showed otherwise.

4.6 Rheological Characterization of the Ferrofluids

Figure 5 shows the magnetic field dependent magnetoviscous effect of both FF-A and FF-B. FF-A shows a slight dependence of the viscosity with both the applied magnetic field and shear rate. Initially, with no magnetic field, FF-A behaves as a Newtonian fluid (shear rate independent of viscosity). As the applied magnetic field increases this behavior is conserved until a threshold magnetic field of approximately 40 kA/m, where shear thinning appears. FF-B shows a more pronounced magnetic field and shear rate dependence of the viscosity. Although at zero applied field FF-B shows Newtonian behavior, increasing magnetic field results in increasing viscosity values. It is observed that the measured viscosity increases approximately one and one-half decades from the initial zero magnetic field value. In addition, the threshold magnetic field that causes a transition from Newtonian to shear thinning behavior is decreased in this ferrofluid to approximately 12 kA/m.

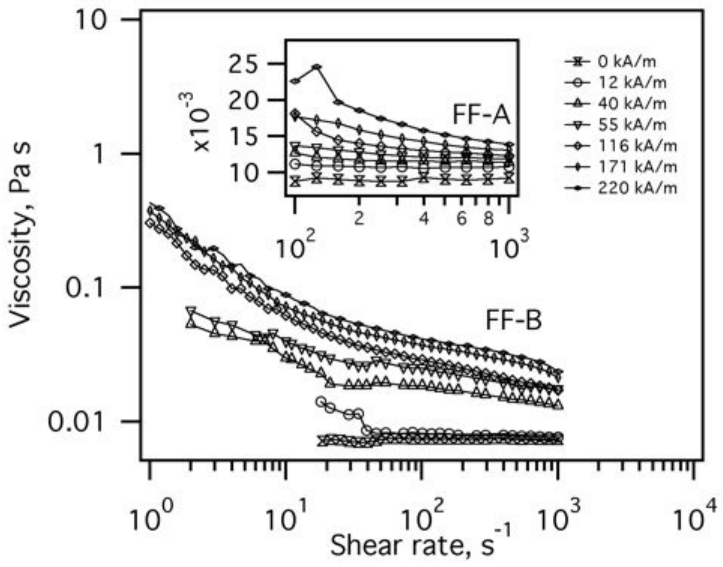

Figure 5. Magnetic field and shear rate dependent viscosity for FF-A and FF-B.

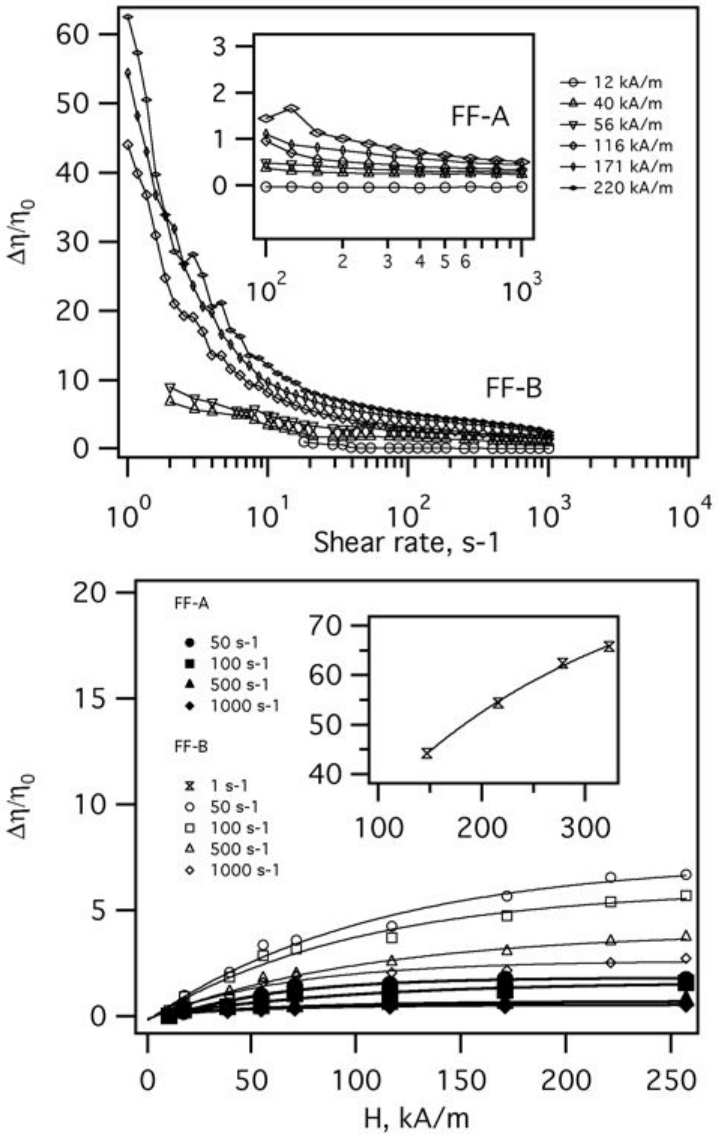

Figure 6. Viscosity change, $\left(\eta_H - \eta_{0,\infty}\right)/\eta_{0,\infty}$, of FF-A and FF-B as a function of shear rate (top) and magnetic field (bottom).

Figure 6 illustrates the viscosity change $\left(\eta_H - \eta_{0,\infty}\right)/\eta_{0,\infty}$ of FF-A and FF-B as a function of shear rate (constant magnetic fields) and magnetic field (constant shear rates). Here η_H is the measured magnetic field dependent viscosity of the ferrofluid, and $\eta_{0,\infty}$ is the measured viscosity of the ferrofluid with zero magnetic field and at large shear rate (1000 s^{-1}). Overall, FF-B shows a greater viscosity change than FF-A, with viscosity changes of 60 fold at low shear rate. When plotting the viscosity change as a function of the applied field (bottom) it is observed that for FF-A viscosity slightly increased with increasing magnetic fields and this effect saturated rapidly. This saturation was also observed in FF-B within the magnetic field range studied here. Decreasing the shear rate resulted in viscosity changes of over 14 fold at low shear rates of 1 s^{-1}. Lower magnetic fields could not be measured due to the low torque limit of the instrument.

Figure 7 illustrates the viscous (loss) and elastic (storage) moduli of FF-A and FF-B as a function of the applied external magnetic field, measured at various constant oscillation frequencies. It is observed that FF-A showed no dependence of the measured viscous modulus with the applied magnetic field. No elastic response in the fluid could be measured within the accuracy of the instrument. FF-B showed measurable viscous and elastic moduli, and both were magnetic field dependent. Moreover, a transition from viscous to elastic behavior occurs above an applied frequency of 10 rads/s, where the storage modulus is higher than the loss modulus, indicating that the elasticity of the fluid dominates it's dynamic rheological behavior. This elastic behavior is conserved throughout the entire applied magnetic field range.

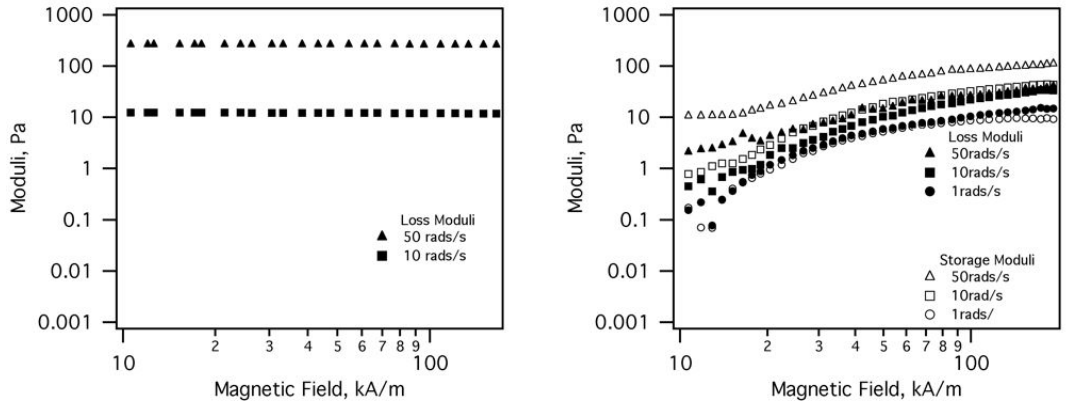

Figure 7. Magnetic field dependent moduli measured at various constant oscillatory frequencies for FF-A (Left) and FF-B (Right).

The Mason number (Mn) is commonly used in interpreting the rheology of magnetic field responsive fluids since it combines various important parameters (e.g. magnetic field, shear rate, solvent viscosity, particle magnetization, etc.) into a single dimensionless number which describes the balance of viscous and magnetic forces. We have used a previously reported Mason number [34], $Mn = \eta_0\dot{\gamma}/2\mu_0\mu_c H^2$, to apply dimensionless treatment of the rheological data. In *Mn*, η_0 is the solvent viscosity, $\dot{\gamma}$ is the shear rate and $\beta = (\chi - 1)/(\chi - 2)$ is the magnetic contrast, where χ is the relative permeability of the particles. The relative permeability was calculated from,

$$\chi = 1 + \frac{M_d}{L(\alpha)} H \tag{2}$$

where $L(\alpha) = \coth\alpha - 1/\alpha$ is the Langevin function, and α is the Langevin parameter. **Figure 8** illustrates the viscosity change as a function of the Mn for the data in **Figure 6**.

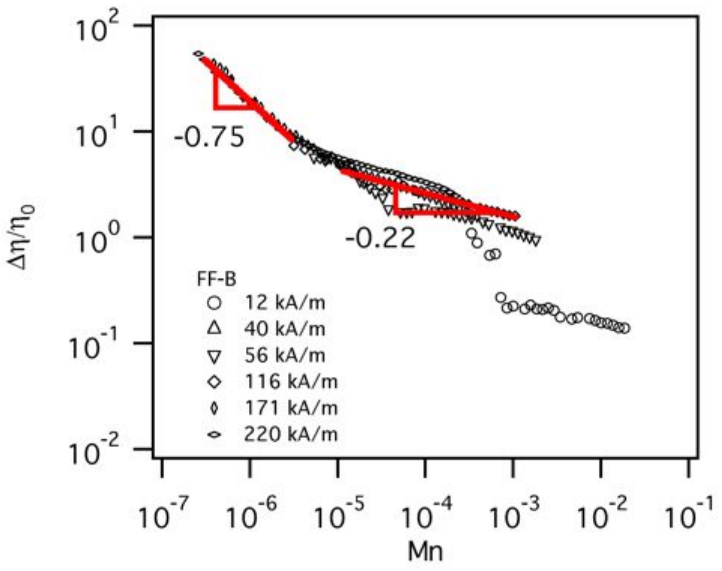

Figure 8 Viscosity change of FF-A and FF-B as a function of the Mason number.

The Mason number did not satisfactorily collapse the viscosity curves of FF-A , however curves for FF-B did collapse for low Mn values. FF-A showed only one decade spread of Mn, whereas FF-B was characterized over almost five decades of Mn. The low values of the Mn are due to the low viscosity of the suspending fluid. FF-B showed two distinct regions of collapse, with two different slopes, the first one being 0.7, which is consistent with spheroidal aggregates at low Mn's in inverse FFs [35], and the second being 0.2, a value that has not been reported for the magnetorheology of FFs.

4.7 Conclusions

The magnetic, structural and magnetorheological properties of well stabilized (FF-A) and poorly stabilized (FF-B) magnetite FFs were investigated. Calculation of the interaction parameter for both fluids resulted in low interactions $(\lambda \approx 1)$, however light scattering and microscopy measurements of the particles showed large particle chains for the ferrofluid having poorly stabilized particles, whereas no chian of particles resulted in the well stabilized ferrofluid. Both fluids followed Langevin magnetization behavior even though earlier reports indicated that aggregated magnetic fluids show deviations from the Langevin function. We have shown that particle stabilization is a variable that may be tuned for increasing the particle interaction without affecting the bulk magnetic properties such as particle magnetization. However tuning the particle stabilization did affect the FFs magnetorheological response, by increasing noticeably the magnetoviscous effect and inducing a yield stress and elastic response when particles were allowed to interact.

4.8 References

1. Rosensweig, R.E., *Ferrohydrodynamics*. 1997, New York: Dover Publications, Inc.
2. Melle, S., et al., *Microstructure evolution in magnetorheological suspensions governed by Mason number*. Physical Review E, 2003. **68**(4): p. 11.
3. Odenbach, S., *Magnetoviscous Effects in Ferrofluids*. 2002, Berlin: Springer.
4. Zubarev, A.Y. and L.Y. Iskakova, *On the theory of phase transitions in magnetic fluids*. Journal of Experimental and Theoretical Physics, 2007. **105**(5): p. 1018-1034.
5. Ivanov, A.O., Z.W. Wang, and C. Holm, *Applying the chain formation model to magnetic properties of aggregated ferrofluids*. Physical Review E, 2004. **69**(3): p. 6.
6. Degennes, P.G. and P.A. Pincus, *Pair Correlations In a Ferromagnetic Colloid*. Physik Der Kondensiterten Materie, 1970. **11**(3): p. 189-+.
7. Zubarev, A.Y. and L.Y. Iskakova, *Theory of physical-properties of magnetic liquids with chain aggregates*. Zhurnal Eksperimentalnoi I Teoreticheskoi Fiziki, 1995. **107**(5): p. 1534-1551.
8. Satoh, A., et al., *Two-dimensional Monte Carlo simulations to capture thick chainlike clusters of ferromagnetic particles in colloidal dispersions*. Journal of Colloid and Interface Science, 1996. **178**(2): p. 620-627.
9. Ilg, P. and S. Hess, *Nonequilibrium dynamics and magnetoviscosity of moderately concentrated magnetic liquids: A dynamic mean-field study*. Zeitschrift Fur

Naturforschung Section a-a Journal of Physical Sciences, 2003. **58**(11): p. 589-600.

10. Huang, J.P., Z.W. Wang, and C. Holm, *Structure and magnetic properties of mono- and bi-dispersed ferrofluids as revealed by simulations*. Journal of Magnetism and Magnetic Materials, 2005. **289**: p. 234-237.
11. Gazeau, F., et al., *Anisotropy of the structure factor of magnetic fluids under a field probed by small-angle neutron scattering*. Physical Review E, 2002. **65**(3).
12. Pop, L., et al., *Microstructure and rheology of ferrofluids*. Journal of Magnetism an Magnetic Materials, 2005. **289**: p. 303-306.
13. Puntes, V.F., K.M. Krishnan, and A.P. Alivisatos, *Colloidal nanocrystal shape and size control: The case of cobalt*. Science, 2001. **291**(5511): p. 2115-2117.
14. Sun, S.H. and C.B. Murray, *Synthesis of monodisperse cobalt nanocrystals and their assembly into magnetic superlattices (invited)*. Journal of Applied Physics, 1999. **85**(8): p. 4325-4330.
15. Butter, K., et al., *Direct observation of dipolar chains in ferrofluids in zero field using cryogenic electron microscopy*. Journal of Physics-Condensed Matter, 2003. **15**(15): p. S1451-S1470.
16. Butter, K., A.P. Philipse, and G.J. Vroege, *Synthesis and properties of iron ferrofluids*. Journal of Magnetism and Magnetic Materials, 2002. **252**(1-3): p. 1-3.
17. Klokkenburg, M., et al., *Direct Imaging of zero-field dipolar structures in colloidal dispersions of synthetic magnetite*. Journal of the American Chemical Society, 2004. **126**(51): p. 16706-16707.

18. Odenbach, S., *Ferrofluids - magnetically controlled suspensions*. Colloids and Surfaces a-Physicochemical and Engineering Aspects, 2003. **217**(1-3): p. 171-178.

19. Odenbach, S., T. Rylewicz, and M. Heyen, *A rheometer dedicated for the investigation of viscoelastic effects in commercial magnetic fluids*. Journal of Magnetism and Magnetic Materials, 1999. **201**: p. 155-158.

20. Odenbach, S., *Ferrofluids, Magnetically Controllable Fluids and Their Applications*. 1 ed. 2002, Berlin: Springer.

21. Odenbach, S. and H. Stork, *Shear dependence of field-induced contributions to the viscosity of magnetic fluids at low shear rates*. Journal of Magnetism and Magnetic Materials, 1998. **183**: p. 188-194.

22. Shahnazian, H. and S. Odenbach, *Yield stress in ferrofluids?* International Journal of Modern Physics B, 2007. **21**(28-29): p. 4806-4812.

23. Ghasemi, E., A. Mirhabibi, and M. Edrissi, *Synthesis and rheological properties of an iron oxide ferrofluid*. Journal of Magnetism and Magnetic Materials, 2008. **320**(21): p. 2635-2639.

24. Hong, R.Y., et al., *Rheological properties of water-based Fe3O4 ferrofluids*. Chemical Engineering Science, 2007. **62**(21): p. 5912-5924.

25. Barrera, C., et al., *Monitoring gelation using magnetic nanoparticles*. Soft Matter. **6**(15): p. 3662-3668.

26. Bhargavi, R., et al., *Enhanced Frank elasticity and storage modulus in a diamagnetic liquid crystalline ferrogel*. Soft Matter, 2011. **7**: p. 10151-10161.

27. Xu, Y.G., et al., *A high-performance magnetorheological material: preparation, characterization and magnetic-mechanic coupling properties*. Soft Matter. **7**(11): p. 5246-5254.

28. Kittipoomwong, D., D.J. Klingenberg, and J.C. Ulicny, *Dynamic yield stress enhancement in bidisperse magnetorheological fluids*. Journal of Rheology, 2005. **49**(6): p. 1521-1538.

29. Viota, J.L., J.D.G. Duran, and A.V. Delgado, *Study of the magnetorheology of aqueous suspensions of extremely bimodal magnetite particles*. European Physical Journal E, 2009. **29**(1): p. 87-94.

30. Ulicny, J.C., et al., *Enhancing magnetorheology with nonmagnetizable particles*. Applied Physics Letters. **96**(23): p. 3.

31. Zubarev, A.Y., *Rheological properties of polydisperse magnetic fluids. Effect of chain aggregates*. Journal of Experimental and Theoretical Physics, 2001. **93**(1): p. 80-88.

32. Chantrell, R.W., et al., *Agglomerate formation in a magnetic fluid*. Journal of Applied Physics, 1982. **53**(3): p. 2742-2744.

33. Ramos, J., J. de Vicente, and R. Hidalgo-Alvarez, *Small-Amplitude Oscillatory Shear Magnetorheology of Inverse Ferrofluids*. Langmuir. **26**(12): p. 9334-9341.

34. Marshall, L., C.F. Zukoski, and J.W. Goodwin, *EFFECTS OF ELECTRIC-FIELDS ON THE RHEOLOGY OF NON-AQUEOUS CONCENTRATED SUSPENSIONS*. Journal of the Chemical Society-Faraday Transactions I, 1989. **85**: p. 2785-2795.

35. Halsey, T.C., J.E. Martin, and D. Adolf, *Rheology of electrorheological fluids*. Physical Review Letters, 1992. **68**(10): p. 1519-1522.

5 Enhanced rheological properties of dilute suspensions of magnetic nanoparticles in a concentrated amphiphilic surfactant solution.

5.1 Abstract

We present an experimental study of the magnetorheological response of a dilute suspension of magnetic nanoparticles in a concentrated amphiphilic surfactant solution. Low particle content (0.4 % v/v) induced significant viscosity increase, of almost six decades, enhancing the shear thinning behavior observed in the absence of the particles. A magnetic field induced yield stress of up to 10 Pa at magnetic fields of up to 0.4 T was also observed. Experiments under small amplitude oscillatory shear indicate a transition from viscous to elastic behavior at a critical magnetic field which depends on the frequency of the oscillatory shear. At low applied magnetic fields both moduli are independent of the magnetic field and increase with the frequency of the oscillatory shear. At high applied magnetic fields both the loss and storage modulus seem to asymptote to a power law dependence on the magnetic field magnitude. These results illustrate the possibility of inducing dramatic changes in the rheological properties of complex fluids by addition of minute amounts of magnetic nanoparticles and application of magnetic fields.

5.2 List of Figures

5.3 List of Tables

5.4 Introduction

The combination of soft materials such as polymers, gels, and associating fluids with inorganic particles has attracted attention in recent years due to an interest in controlling their fluid properties. One such example is magnetic responsive soft materials which have attracted interest due to the possibility of modulating complex fluid response through application of magnetic fields. These materials consist of incorporating small amounts of colloidally stable magnetic nanoparticles within the matrix of a complex fluid. Examples of magnetic soft materials include ferrogels [1] and ferronematics [2]. These magneto-responsive complex fluids represent a new kind of fluid which combine the unique magnetic properties of the dispersed magnetic nanoparticles with those of the soft material matrix, including viscoelasticity, yield stresses, and time dependent rheological behavior.

When a magnetic field is applied to a suspension of magnetic nanoparticles in a Newtonian fluid, a so-called ferrofluid, a reversible increase in viscosity results due to the alignment of the magnetic dipoles of the nanoparticles in the direction of the applied magnetic field. This is known as the magnetoviscous effect [3]. The rheological properties of ferrofluids in magnetic fields have been studied in detail [3-19], however the rheological properties of magnetic soft materials has received little attention. For example, incorporation of small amounts of magnetite nanoparticles in a lyotropic polymer liquid crystalline matrix (a ferronematic) [20] and in a liquid crystalline ferrogel [21] resulted in an enhanced viscosity. In ferrogels, the rheological properties are potentially interesting due to the known elastic nature of the gel matrix. Coupling of the

elastic response of the gel with the magnetic response of the nanoparticles is attractive for various applications, such as in drug carriers [22, 23], artificial muscles [24], and cancer therapeutics [25]. Elongation, contraction and curvature can be induced in this type of magnetic soft material [1]. Also, enhancements in elastic behavior with applied magnetic field have been reported [26-31]. It is important to emphasize that these novel magneto-responsive soft materials consist of small amounts of magnetic content, typically in the order of 10-30 % by wt. However, dramatic changes in the properties of these materials may result even with addition of such small amounts of particles.

Amphiphilic surfactant molecules consist of hydrophilic (head) and lyophilic (tail) groups bonded together and in solution self-assemble into aggregates such as spheroidal micelles, vesicles, bilayers [32], and even into nematic liquid crystals and gels at high enough concentrations [33]. Applications of such materials are motivated by their ability to self-reassemble after flow disrupts their structure. Applications range from detergents and emulsifiers to viscosifiers and drag reducing agents. It has been reported that spherical surfactant micelles yield low viscosities even at high concentrations [34]. On the other hand, rod-like micelles result in highly viscous solutions and viscoelasticity appears even at low concentrations [35]. Finally, vesicles with solvent encapsulated in their interior, result in densely packed highly viscous fluids, exhibiting yield stresses [36]. The possibility of modulating the rheological properties of amphiphilic surfactant solutions by addition of magnetic nanoparticles and application of magnetic fields appears unexplored.

Here is reported a magnetic soft material consisting of dilute suspensions of cobalt ferrite nanoparticles in a concentrated oleic acid surfactant/mineral oil mixture. We

call this soft material a Magnetic Concentrated Amphiphilic Surfactant Solution (MCASS). The magnetic response of this material was characterized with respect to the effect of magnetic fields on rheological behavior. This magnetic soft material with a small amount of magnetic content shows strong magnetorheological behavior, magnetic field induced yield stresses, and viscoelastic behavior which are not observed in the absence of the nanoparticles.

5.5 Materials and Methods

5.5.1 Materials

The mineral oil used was obtained commercially. The oleic acid (99%), iron (III) chloride hexahydrate ($FeCl_3 \cdot 6H_2O$), and cobalt (II) chloride hexahydrate ($CoCl_2 \cdot 6H_2O$) were obtained from Sigma Aldrich. Sodium oleate and 1-Octadecene were obtained from Fisher Scientific. All materials were used as received.

5.5.2 Sample Preparation

Concentrated Amphiphilic Surfactant Solutions (CASS's). The concentrated amphiphilic surfactant solutions consisted of oleic acid dissolved in mineral oil. These were prepared by mixing previously calculated amounts of both materials in a glass vial, followed by agitation with a magnetic stirrer at ambient temperature for 30 minutes. Samples prepared ranged from 10%wt to 95%wt of oleic acid in mineral oil. Afterwards the samples were left to rest and characterization was performed one week later. The CMC (critical micelle concentration) of oleic acid is reported to range from 0.72mM to 3.5mM [37], therefore the concentrated surfactant solutions used here likely had self assembled surfactant structures.

Magnetic nanoparticle synthesis. The particles used to prepare the MCASS's were oleic acid coated cobalt ferrite nanoparticles. These were synthesized by the thermal-decomposition method [38]. First a metal-oleate precursor ($Co^{+2}Fe^{+3}$) was synthesized by

dissolving 20 mmol of $FeCl_3 \cdot 6H_2O$, 10 mmol of $CoCl_2 \cdot 6H_2O$, and 80 mmol of sodium oleate in a mixture of ethanol, distilled water, and hexane under reflux at 70ºC for 4 hours. The resulting mixture consisted of two phases, an organic phase containing the metal-oleate and an aqueous phase containing the salts. These were separated by adding distilled water in a separation funnel. The metal-oleate obtained was stored in a vacuum oven at 70ºC overnight for evaporation of the ethanol and hexane. The cobalt ferrite particle synthesis used 25 g of this metal-oleate mixed with 0.08 M of oleic acid in 1-Octadecene. This mixture was then heated to 320ºC at a rate of 3.3ºC/min followed by reaction at this temperature for 3 hours. After this when the mixture had reached ambient temperature the resulting colloidal suspension consisted of the oleic acid coated cobalt ferrite particles. The resulting colloidal suspension was then centrifuged with acetone in a 1:3 mixture proportion at 8500 rpm for 15 minutes. This was repeated three times. After this a waxy-magnetic material was obtained.

Magnetic Concentrated Amphiphilic Surfactant Solutions (MCASS's). The magnetic concentrated amphiphilic surfactant solutions were prepared by adding previously calculated amounts of particles to the oleic acid/mineral oil solutions. Two MCASS's were prepared, both in a 70%wt oleic acid/mineral oil mixture, but with different particle concentrations and labeled MCSS-A and MCSS-B. The particles used where obtained from two synthesis batches. After the particles were added to the oleic acid/mineral oil mixtures, the solutions were agitated mechanically followed by sonication for five minutes. Samples were stored at ambient temperature. No precipitation was observed during the subsequent experiments over a period of 6 months.

5.5.3 Sample Characterization

The hydrodynamic diameter of the cobalt ferrite particles was measured using a Brookhaven Instruments BI 90-Plus Dynamic Light Scattering particle size analyzer. The particles were suspended in *n*-hexane in a glass couvette at ambient temperature. Samples were filtered using Teflon filters (PTFE 0.4μm) before each measurement. The core nanoparticle size was measured in a Carl Zeiss Leo 922 Transmission Electron Microscope operated at 200kV. Particles were first suspended in hexane and then deposited onto carbon coated grids. Afterwards the hexane was left to evaporate by placing the grid in a vacuum oven set to 70ºC for 1 hour.

The magnetic response of the MCASS's was measured using a Quantum Design MPMS XL-7 Superconducting Quantum Interference Device (SQUID) Magnetometer. Magnetization curves were measured at 300 K. AC susceptibility measurements were performed at 273K.

Rheological measurements of the samples were performed using an Anton Paar Physica MCR 301 series rheometer with a Magnetorheological Device (MRD). This device applies magnetic fields normal to the applied shear deformation. We used a 20 mm cone-plate fixture with a 0.02 mm gap. With this attachment a current is set by the user and the magnetic field is generated in the coil. A Magnet-Physik FH 54 Gauss-Tesla meter (Hall probe) positioned below the stationary lower plate allows for measurement of the magnetic field of the sample while the rheological measurements are made. The sample temperature was controlled using a thermocouple, also placed below the lower plate, and a feedback control loop using a Julabo F25 water/ethanol bath. Sample loading was performed in the following manner. First the sample was loaded onto the lower

stationary plate of the rheometer followed by lowering the upper plate until a gap height of 0.02 mm was reached. After this, a pre-shear of 100 s^{-1} was applied. Afterwards the sample was left to relax for 5 minutes before any measurement was performed. Steady state viscosity curves were measured by applying a constant shear rate and magnetic field and measuring the viscosity until a steady state value was achieved at each shear rate. Measurements were done with decreasing shear rate until the measured torques were at the detection limit of the instrument (10^{-4} mN m). A constant magnetic field was applied throughout. Then a new curve was obtained by starting at high shear with a new magnetic field. The yield stress curves were measured by applying a logarithmic shear stress ramp and measuring the viscosity while applying a constant magnetic field. Oscillatory rheometry measurements were performed by applying a logarithmic increasing magnetic field while measuring the storage and loss moduli at various fixed frequencies. Again, all samples were first pre-sheared before any rheological measurements.

5.5 Results and Discussion

Figure 1 shows the hydrodynamic size distributions of the cobalt ferrite particles used to prepare the magnetic concentrated amphiphilic surfactant solutions MCASS-A and MCASS-B. The particles show hydrodynamic sizes of 20 nm and 19 nm, respectively.

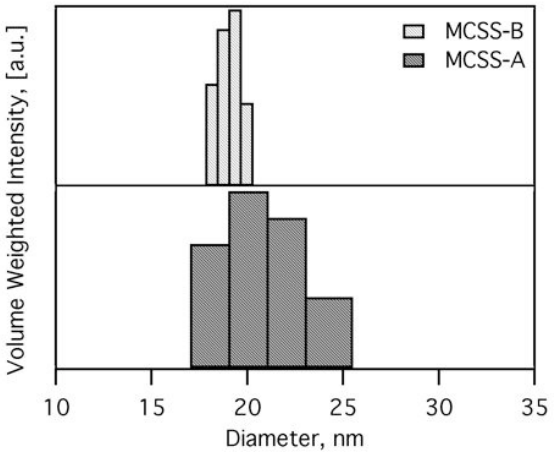

Figure 1. Hydrodynamic size distribution of the oleic acid coated cobalt ferrite nanoparticles used for samples MCASS-A and MCASS-B. Nanoparticles suspended in *n*-hexane.

Figure 2 shows TEM images of the particles used for preparing MCSS-A and MCSS-B samples. Size distribution analysis resulted in a diameter of 15$\pm$1.87 nm for MCASS-A and 12$\pm$1.52 nm for MCASS-B.

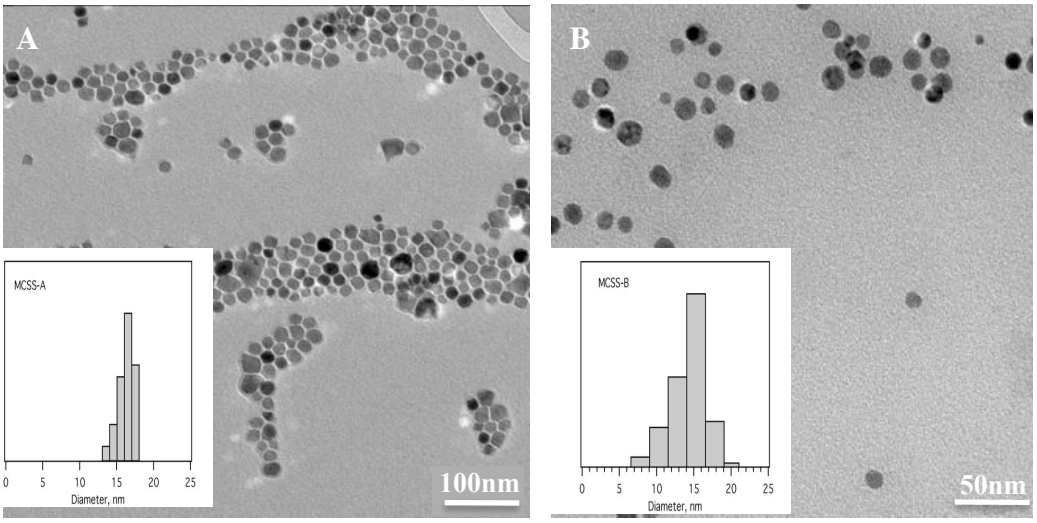

Figure 2. Transmission electron microscopy of the cobalt ferrite magnetic nanoparticles used for MCASS-A and MCASS-B.

Figure 3 shows the equilibrium magnetization curves of MCASS-A and MCASS-B measured at 300K (top), both showing typical superparamagnetic behavior. Initially, application of an increasing magnetic field results in linear magnetization, followed by saturation at high fields. Markers correspond to the raw data, while the solid line corresponds to a nonlinear fit to the Langevin function weighted by the lognormal size distribution,

$$M = \int_0^\infty M_s \left[\coth \alpha\left(H, D_m\right)\right] n_v\left(D_m\right) dD_m \tag{1}$$

where M is the magnetization of the suspension at an applied magnetic field M, M_s is the saturation magnetization, and $\alpha\left(H, D_m\right)$ is the Langevin parameter. The Langevin parameter is given by

$$\alpha\left(H, D_m\right) = \frac{\mu_0 \pi M_d H D_m^3}{6 k_B T} \tag{2}$$

where μ_0 is the permeability of free space, M_d is the domain magnetization (446 kA/m [39]), k_B is Boltzman's constant, and T is the temperature. The volume weighted lognormal distribution is given by

$$n_v\left(D_m\right) = \frac{1}{\sqrt{2\pi} D_m \ln \sigma} \exp\left(-\frac{\ln^2 D_m / D_{mgv}}{2 \ln^2 \sigma_g}\right) \tag{3}$$

where D_{mvg} is the volume mean magnetic diameter and $\ln \sigma_g$ is the geometric deviation of the distribution. The particle magnetic diameters were 8 nm ($\ln \sigma_g$ = 1.36) for

MCASS-A and 9 nm ($\ln\sigma_g$=0.46) for MCASS-B. The volume fractions were 0.4% v/v for MCASS-A and 0.06 % v/v for MCASS-B. MCASS-A being slightly more concentrated it had a slightly higher saturation magnetization than MCASS-B.

Figure 3 also shows the AC susceptibility response when an oscillating magnetic field is applied. The Brownian relaxation of the particles is demonstrated by the peak of the out-of-phase component of the susceptibility, where $\Omega\tau_B = 1$. This allows for calculation of the experimental Brownian relaxation times of the particles, which were 0.7 ms for MCASS-A and 0.5 ms for MCSS-B. A theoretical Brownian relaxation time of magnetic nanoparticles was calculated using [39]:

$$\tau_B = \frac{3\eta V_H}{k_B T} \tag{4}$$

where η is the carrier fluids viscosity, V_H is the volume of the particles calculated using the hydrodynamic diameter measured with the dynamic light scattering, k_B is Boltzmans' constant, and T is the absolute temperature, resulting in 2.7 ms for MCASS-S and 2.3 ms for MCASS-B. Results are shown in **Table 1**. We have used the viscosity of mineral oil as the carrier fluids viscosity.

Table 1. Measured hydrodynamic diameter of MCASS-A and MCASS-B, with the experimental and theoretical calculation of the Brwonian relaxation time.

	D_H , nm	$\tau_{B,theory}$, ms	τ_{exp} , ms
MCASS-A	20	2.7	0.7
MCASS-B	19	2.3	0.5

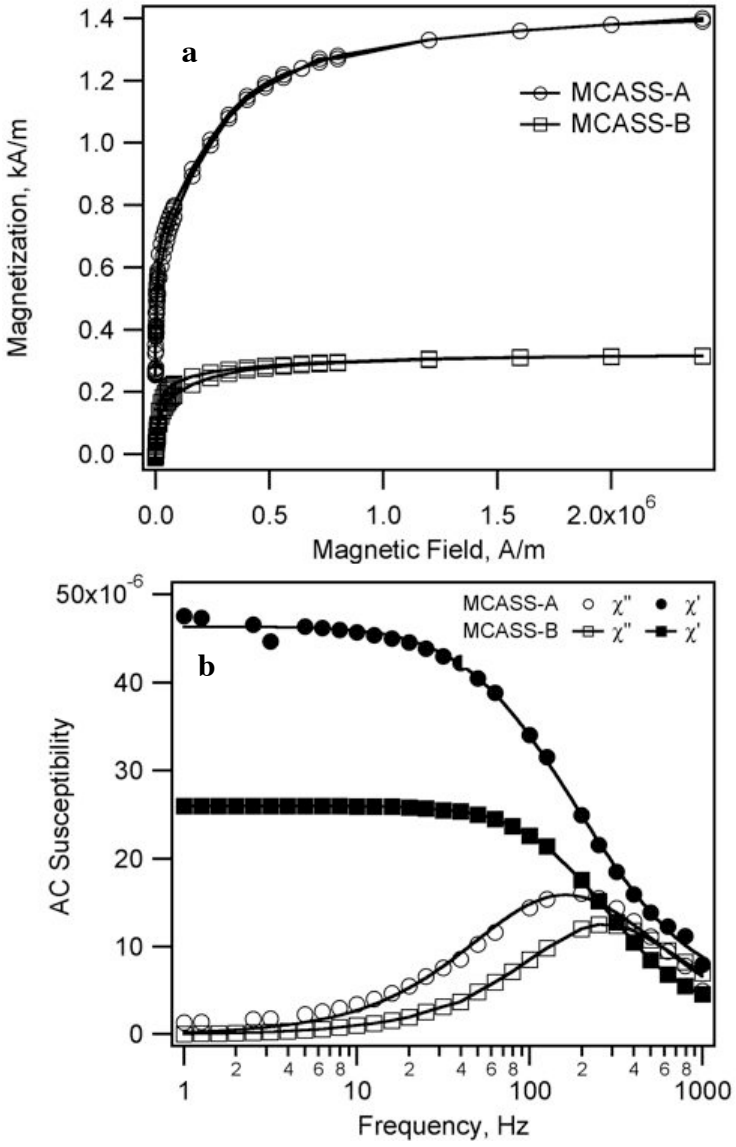

Figure 3. Magnetic characterization of MCASS-A and MCASS-B. (a) Equilibrium magnetization curve. (b) AC susceptibility measured as a function of the applied magnetic field frequency.

Figure 4 shows the steady state viscosity response of the MCASS-A and MCASS-B samples as a function of the applied shear rate and magnetic field. Additionally, the viscosity of oleic acid/mineral oil solutions of varying concentrations are shown in the inset. It is observed that neat oleic acid and neat mineral oil show Newtonian behavior, with mineral oil being slightly more viscous than the oleic acid. Addition of varying amounts of oleic acid to the mineral oil results in a decrease in viscosity as the amount of oleic acid increases. Moreover, at low shear rates shear thinning results at 90% wt oleic acid fractions, which suggests formation and breakup of oleic acid structures resulting in non-Newtonian behavior.

Addition of the small amounts of magnetic nanoparticles used in MCASS-A and MCASS-B to the 70%wt oleic acid/mineral oil resulted in a slight increase in viscosity at high shear rates, with the effect being greater for MCASS-A owing to the slightly higher concentration of particles. Interestingly, MCASS-A and MCASS-B without magnetic fields show shear thinning behavior. Application of an external magnetic field intensifies this shear thinning behavior, and also shifts the high shear rate plateau towards higher shear rates. This magnetic field dependent viscosity response is similar to the magnetoviscous effect observed in ferrofluids (*i.e.* magnetic nanoparticle suspensions in a Newtonian fluid), although here a complex carrier fluid is used resulting in an enhanced viscosity of almost 2.5 orders in magnitude at low shear rates, where the magnetic field effect is greater, and using only minute amounts of nanoparticles.

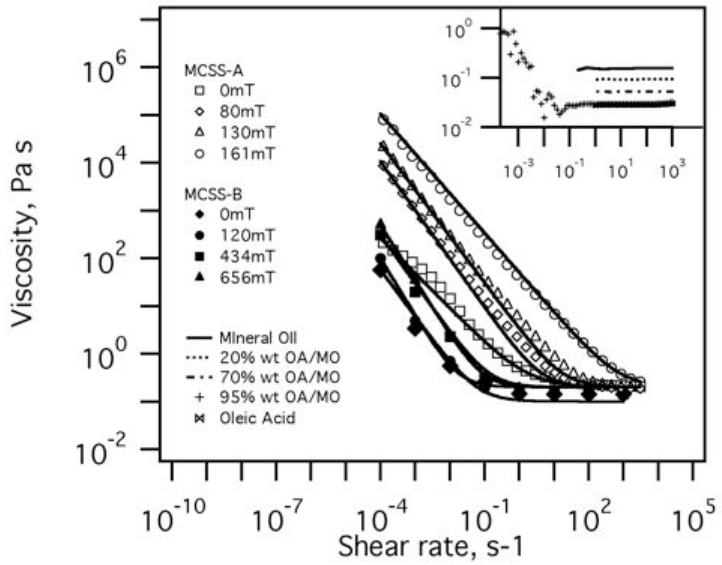

Figure 4. Magnetic field and shear rate dependent viscosity of the magnetic concentrated amphiphilic surfactant solutions A (open symbols) and B (closed symbols) as a function of the applied shear rate measured at constant applied magnetic fields. Inset corresponds to mineral oil with varying amounts of oleic acid.

Table 2. Fitting parameters used for viscosity curves in Figure 4.

MCSS-A			
H, mT	*c*, Pa s^2	n	η_∞, Pa s
161	50	0.83	0.259
130	3.23	0.97	0.189
80	0.89	1.1	0.188
0	0.2	0.73	0.206
MCSS-B			
H, mT	*c*, Pa s^2	n	η_∞, Pa s
656	0.011	1.16	0.154
434	0.025	1.02	0.148
120	0.0015	1.2	0.16
0	0.0062	0.99	0.1445

The magnetic field dependent viscosity shown in Figure 4 follows power law behavior, and the solid lines correspond to fitting to the formula,

$$\eta = c\dot{\gamma}^{-n} + \eta_{\infty} \tag{5}$$

where *c, n,* and η_{∞} are fitting constants, the latter corresponding to the high-shear rate viscosity. The obtained fitting constants are presented in **Table 2**. The parameter *n* ranged from 0.7 to 1.2, which is higher than values reported for other magnetic fluids such as inverse ferrofluids (0.6 to 0.8) [18]. We see that *n* is not significantly magnetic field dependent.

Figure 5 shows the measured loss and storage moduli of the MCASS-A as a function of the applied magnetic field, at various frequencies. A crossover of the moduli occurs at a threshold magnetic field for each fixed frequency. Before the crossover at all frequencies the loss modulus is higher in magnitude than the storage modulus, meaning that the sample behaves as a viscous fluid. Above the threshold magnetic field the storage modulus is higher than the loss modulus and the fluid behaves elastically. The storage modulus and loss modulus had power law dependencies of 0.33 ± 0.01 and 0.67 ± 0.01 with the magnetic field, these were obtained by fitting the curves in the high magnetic field region. The threshold magnetic field for moduli crossover had a 0.31 ± 0.01 power dependence with the applied oscillatory frequency. Similar measurements were also performed on the oleic acid/mineral oil mixtures, where no magnetic field dependent behavior or storage modulus were observed.

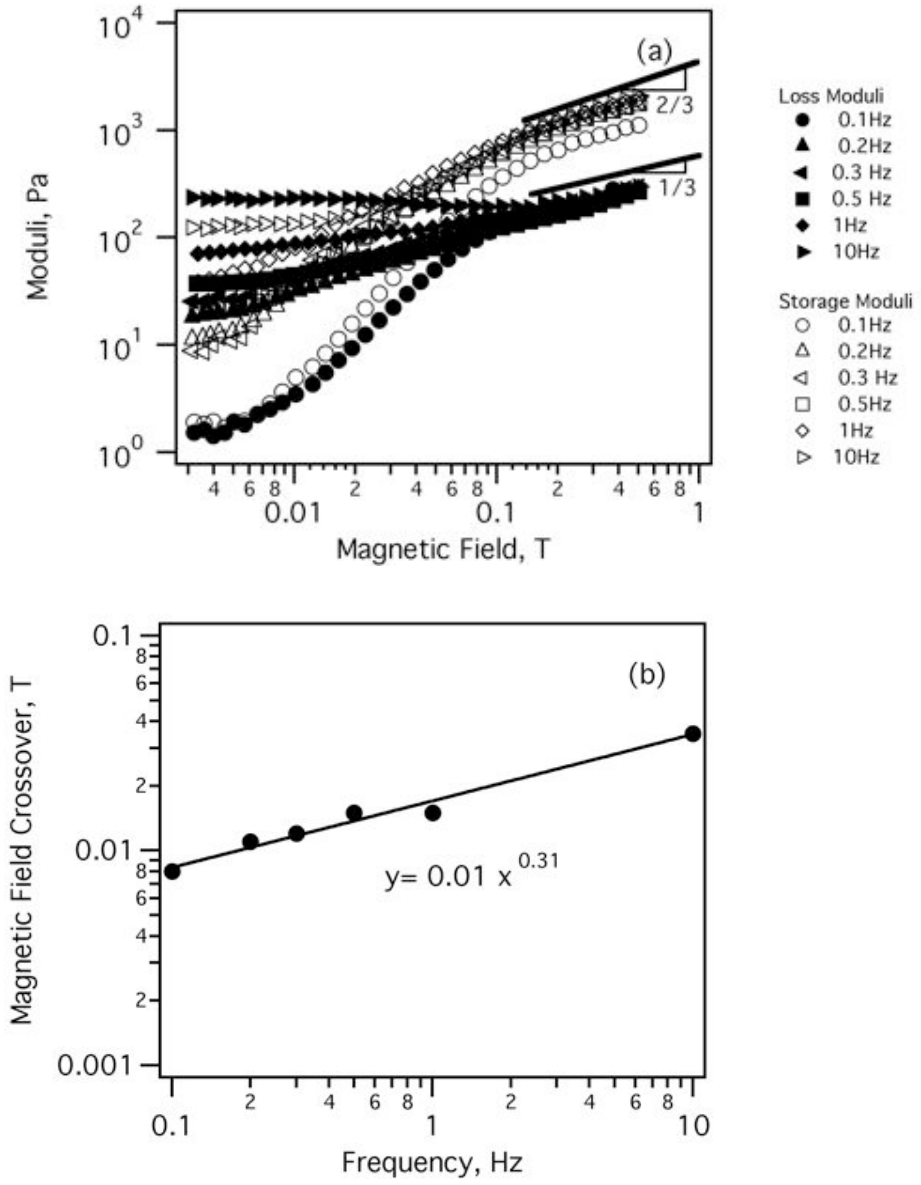

Figure 5. (a) Oscillatory moduli of the soft magnetic fluid MCASS-A measured with an increasing magnetic field at various frequencies. (b) Frequency dependence of the critical magnetic field for moduli crossover in (a).

Figure 6 shows the measured viscosity as a function of the applied stress at constant applied magnetic fields, used to determine the yield stresses of MCASS-A. The yield stress is the minimum applied stress needed for the sample to flow. Typically, a yield stress is associated with a sudden marked decrease in the measured viscosity. It is observed that initially when no magnetic nanoparticles are present a 70%wt mixture of oleic acid/mineral oil shows a subtle yield stress near 0.01 Pa. Addition of the 0.4% v/v of magnetic nanoparticles (MCSS-A) shifts this yield stress to approximately 1 Pa in zero field. Application of a magnetic field not only continuously increases the yield stress, but also results in the appearance of a second yield stress. Figure 7 shows the effect of the magnetic field on the measured yield stresses of MCASS-A. It can be observed that the yield stresses of sample MCASS-A are magnetic field dependent and saturate above a magnetic field of 84mT.

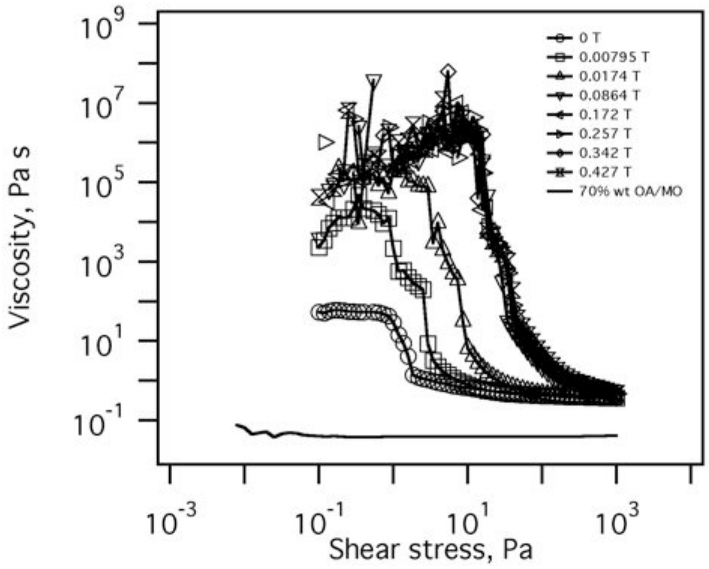

Figure 6. Viscosity of MCASS-A as a function of the applied shear stress.

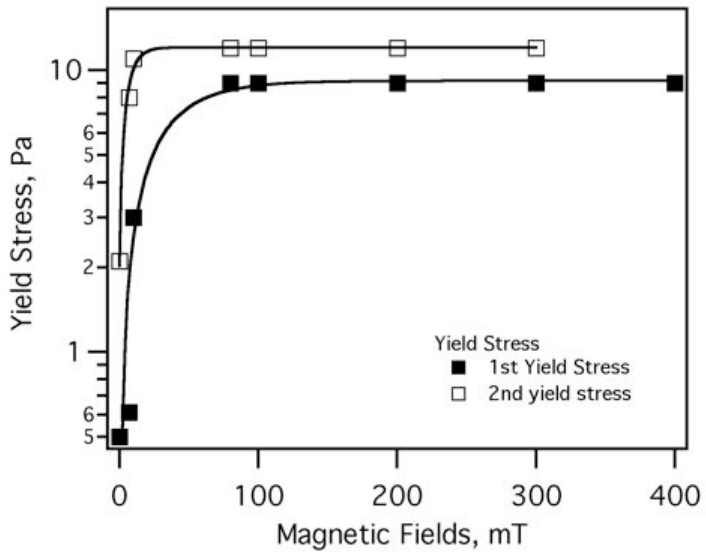

Figure 7. Magnetic field dependent 1st and 2nd yield stresses, obtained from Figure 6.

5.6 Conclusions

We have prepared and characterized a new magnetic soft material consisting of magnetic nanoparticles suspended in a concentrated amphiphilic surfactant solution of oleic acid in mineral oil. Small amounts of particles resulted in magnetic field dependent viscosity increase of over five decades in viscosity with fields of up to 161 mT, and shear thinning with power law dependence on shear rate. The fluid also displayed magnetic field induced yield stresses of up to 10 Pa with applied magnetic fields of up to 0.4 T, and magnetically tuned viscoelastic behavior. These features were not observed in the absence of the nanoparticles, demonstrating the potential of adding minute amounts of magnetic nanoparticles and applying magnetic fields in modulating the rheological properties of complex fluids such as concentrated surfactant solutions.

5.7 References

1. Zrinyi, M., L. Barsi, and A. Buki, *Ferrogel: a new magneto-controlled elastic medium*. Polymer Gels and Networks, 1997. **5**(5): p. 415-427.
2. Burylov, S.V. and Y.L. Raikher, *Magnetic Fredericksz Transition in a Ferronematic*. Journal of Magnetism and Magnetic Materials, 1993. **122**(1-3): p. 62-65.
3. Odenbach, S., *Magnetoviscous Effects in Ferrofluids*. 2002, Berlin: Springer.
4. Hong, R.Y., et al., *Rheological properties of water-based Fe3O4 ferrofluids*. Chemical Engineering Science, 2007. **62**(21): p. 5912-5924.
5. Ilg, P., E. Coquelle, and S. Hess, *Structure and rheology of ferrofluids: simulation results and kinetic models*. Journal of Physics-Condensed Matter, 2006. **18**(38): p. S2757-S2770.
6. McTague, J., *Magnetoviscosity of Magnetic Colloids*. The Journal of Chemical Physics, 1969. **51**(1): p. 133136.
7. Odenbach, S., *Ferrofluids, Magnetically Controllable Fluids and Their Applications*. 1 ed. 2002, Berlin: Springer.
8. Odenbach, S., *Ferrofluids - magnetically controlled suspensions*. Colloids and Surfaces a-Physicochemical and Engineering Aspects, 2003. **217**(1-3): p. 171-178.
9. Odenbach, S., T. Rylewicz, and M. Heyen, *A rheometer dedicated for the investigation of viscoelastic effects in commercial magnetic fluids*. Journal of Magnetism and Magnetic Materials, 1999. **201**: p. 155-158.

10. Odenbach, S. and H. Stork, *Shear dependence of field-induced contributions to the viscosity of magnetic fluids at low shear rates*. Journal of Magnetism and Magnetic Materials, 1998. **183**: p. 188-194.

11. Pop, L., et al., *Microstructure and rheology of ferrofluids*. Journal of Magnetism an Magnetic Materials, 2005. **289**: p. 303-306.

12. Pop, L.M., et al., *The microstructure of ferrofluids and their rheological properties*. Applied Organometallic Chemistry, 2004. **18**(10): p. 523-528.

13. Pop, L.M. and S. Odenbach, *Investigation of the microscopic reason for the magnetoviscous effect in ferrofluids studied by small angle neutron scattering*. Journal of Physics-Condensed Matter, 2006. **18**(38): p. S2785-S2802.

14. Rosensweig, R., R. Kaiser, and G. Miskolcz, *Viscosity of Magnetic Fluid in a Magnetic Field*. Journal of Colloid and Interface Science, 1969. **29**(4): p. 680-&.

15. Shahnazian, H. and S. Odenbach, *Yield stress in ferrofluids?* International Journal of Modern Physics B, 2007. **21**(28-29): p. 4806-4812.

16. Shliomis, M.I., *Effective Viscosity of Magnetic Suspensions*. Soviet Physics Jetp-Ussr, 1972. **34**(6): p. 1291.

17. Viota, J.L., J.D.G. Duran, and A.V. Delgado, *Study of the magnetorheology of aqueous suspensions of extremely bimodal magnetite particles*. European Physical Journal E, 2009. **29**(1): p. 87-94.

18. Volkova, O., et al., *Magnetorheology of magnetic holes compared to magnetic particles*. Journal of Rheology, 2000. **44**(1): p. 91-104.

19. Zubarev, A.Y., *Rheological properties of polydisperse magnetic fluids. Effect of chain aggregates*. Journal of Experimental and Theoretical Physics, 2001. **93**(1): p. 80-88.

20. Santiago-Quinones, D.I., A. Acevedo, and C. Rinaldi, *Magnetic and magnetorheological characterization of a polymer liquid crystal ferronematic*. Journal of Applied Physics, 2009. **105**(7): p. 3.

21. Bhargavi, R., et al., *Enhanced Frank elasticity and storage modulus in a diamagnetic liquid crystalline ferrogel*. Soft Matter, 2011. **7**: p. 10151-10161.

22. Szabo, D., G. Szeghy, and M. Zrinyi, *Shape transition of magnetic field sensitive polymer gels*. Macromolecules, 1998. **31**(19): p. 6541-6548.

23. Liu, T.Y., et al., *Study on controlled drug permeation of magnetic-sensitive ferrogels: Effect of Fe3O4 and PVA*. Journal of Controlled Release, 2008. **126**(3): p. 228-236.

24. Bar-Cohen, Y., *Artificial muscles based on electroactive polymers as an enabling tool in biomimetics*. Proceedings of the Institution of Mechanical Engineers Part C-Journal of Mechanical Engineering Science, 2007. **221**(10): p. 1149-1156.

25. Bohlius, S., H.R. Brand, and H. Pleiner, *Macroscopic dynamics of uniaxial magnetic gels*. Physical Review E, 2004. **70**(6).

26. Varga, Z., G. Filipcsei, and M. Zrinyi, *Smart composites with controlled anisotropy*. Polymer, 2005. **46**(18): p. 7779-7787.

27. Chatterjee, J., Y. Haik, and C.J. Chen, *Biodegradable magnetic gel: synthesis and characterization*. Colloid and Polymer Science, 2003. **281**(9): p. 892-896.

28. Gollwitzer, C., et al., *Measuring the deformation of a ferrogel sphere in a homogeneous magnetic field*. Journal of Chemical Physics, 2008. **128**(16).

29. Raikher, Y.L. and V.V. Rusakov, *Viscoelastic ferrogel: Dynamic magnetic susceptibilities*. Brazilian Journal of Physics, 2001. **31**(3): p. 366-379.

30. Ramanujan, R.V. and L.L. Lao, *The mechanical behavior of smart magnet-hydrogel composites*. Smart Materials & Structures, 2006. **15**(4): p. 952-956.

31. Snyder, R.L., V.Q. Nguyen, and R.V. Ramanujan, *Design parameters for magneto-elastic soft actuators*. Smart Materials & Structures, 2010. **19**(5).

32. Larson, R., *The Structure and Rheology of Complex Fluids*, ed. K.E. Gubbins. 1999, New York: Oxford University Press.

33. Berret, J.F., et al., *Tumbling behavior of nematic worm-like micelles under shear flow*. Europhysics Letters, 1995. **32**(2): p. 137-142.

34. Gradzielski, M., *The rheology of vesicle and disk systems - Relations between macroscopic behaviour and microstructure*. Current Opinion in Colloid & Interface Science. **16**(1): p. 13-17.

35. Rehage, H. and H. Hoffmann, *Viscoelastic surfactant solutions - model systems for rheological research*. Molecular Physics, 1991. **74**(5): p. 933-973.

36. Wanka, G., H. Hoffmann, and W. Ulbricht, *Phase diagrams and aggregation behavior of Poly(oxyethylene)-poly(oxypropylene)-poly(oxyethylene) triblock copolymer in aqueous solutions*. Macromolecules, 1994. **27**(15): p. 4145-4159.

37. Murakami, K., S.Y. Chan, and A. Routtenberg, *Protein-kinase-C activation by cis-fatty acid in the absence of Ca-2+ and phospholipids*. Journal of Biological Chemistry, 1986. **261**(33): p. 5424-5429.

38. Park, J., et al., *Ultra-large-scale syntheses of monodisperse nanocrystals*. Nature Materials, 2004. **3**(12): p. 891-895.

39. Rosensweig, R.E., *Ferrohydrodynamics*. 1997, New York: Dover Publications, Inc.

6 Magnetic and Magneto-Rheological Characterization of a Polymer Liquid Crystal Ferronematic

Abstract

Cobalt Ferrite ($CoFe_2O_4$) nanoparticles of ~12nm diameter were suspended in the polymer liquid crystal (LC) HPC/*m*-cresol to form a new type of ferronematic. Suspension of these particles in 35% wt HPC in *m*-cresol did not affect the appearance of the liquid crystalline phase as evidenced by Small Angle X-Ray Scattering (SAXS). Magnetic measurements performed on the 35% wt HPC/*m*-cresol/$CoFe_2O_4$ ferronematic showed the appearance of ferromagnetic behavior and magnetic hysteresis. In addition rheometry of the samples showed magnetorheological effect upon application of a DC magnetic field, with the ferronematic having the largest response.

6.1 List of Figures

6.2 Introduction

When nanoparticles are suspended in a liquid crystalline matrix changes in physical properties are to be expected. Deformations of the liquid crystal matrix occur due to interactions between suspended fillers and particle/LC interactions, which in effect provoke orientational domains in the liquid crystalline arrangement [1, 2], drastically affecting the properties of the liquid crystal. Moreover response of these filled systems to external applied fields (e.g. electric or magnetic) may result in new physical behavior, as well as formation of self-assembled structures.

Many liquid crystals possess magnetic anisotropy, which allows their orientation with relatively large applied magnetic fields, the so-called Friedericksz transition [3]. This manipulation may become less difficult when magnetic nanoparticles are suspended in the liquid crystal matrix [3], in what is referred to as ferronematics. Suspension of magnetic particles in thermotropic liquid crystals has been studied with respect to the effect on the threshold applied DC magnetic field for the Friedericksz transition. Changes in the threshold magnetic Fredericksz transition may result due to changes in the mesogen-particle alignment and/or interaction energy and due to particle concentration [4, 5]. Also numerical studies have shown that the magnetic field surrounding spherical particles suspended in a nematic liquid crystal may cause defect transitions between hedgehog (point-like) and Saturn ring (encircling line) [6].

Incorporation of magnetic particles in HPC polymer has been studied in development of biodegradable polymer magnetic gels for drug delivery [7] and sensors [8]. On the other hand, fillers such as silica and polystyrene particles have been suspended in HPC liquid crystals. [9,

10]However, suspension of magnetic nanoparticles in HPC liquid crystals has not yet been reported.

It is known that the suspension of magnetic nanoparticles in a non-magnetic carrier liquid, also known as a ferrofluid, results in magneto-responsive Non-Newtonian behavior upon application of external applied magnetic fields [11]. A field dependent magneto-viscous effect should in principle also be observed in polymer liquid crystals (i.e. without magnetic particles), as recent modeling studies indicate the possibility of magnetic field induced alignment of the director field under flow [12]. Despite this, the magneto-viscous effect observed in ferrofluids has not yet been reported in polymer liquid crystals or in ferronematics. Herein we present the first observations of a magnetoviscous effect in the polymer liquid crystal HPC/*m*-cresol and a cobalt ferrite/HPC/*m*-cresol based ferronematic.

6.3 Materials and Methods

6.3.1 Materials

HPC (100,000 MW according to manufacturer) was obtained from Sigma Aldrich, and dried for 24 hrs prior to sample preparation. The solvent *m*-cresol was also obtained from Sigma-Aldrich and filtered under vacuum using PTFE filters. HPC in *m*-cresol forms liquid crystalline phases above 23% wt HPC[13]. Cobalt ferrite ($CoFe_2O_4$) nanoparticles were obtained from Ferrotec.

Polymer liquid crystal samples were prepared by adding the dried HPC to the filtered *m*-cresol. For the polymer liquid crystal ferronematic samples the magnetic nanoparticles were first suspended in *m*-cresol and then the HPC was added. Particles were suspended at a concentration of approximately 0.007 % v/v of nanoparticles in HPC/*m*-cresol solution.

Samples were prepared with 15 and 35% w/w HPC in *m*-cresol, stored in a dessicator and kept at ambient temperature for 3 months before any characterization was performed. For the first month, samples were mixed mechanically at least once per week.

6.3.2 Characterization

Particle hydrodynamic diameter was determined using a Brookhaven Instruments BI 90-Plus particle size analyzer. Particles were suspended in *m*-cresol and hexane, filtered with 0.4μm PTFE filters 3 times, and analyzed at 25^{o}C.

The appearance of a liquid crystalline phase with increasing concentration of HPC was confirmed through Small Angle X-Ray Scattering (SAXS) using a Rigaku Ultima II X-Ray Diffractometer with SAXS attachment. Aqueous liquid crystalline HPC shows a characteristic peak at a scattering vector value of 0.4 Å^{-1}, changes in this peak upon suspension of particles may indicate distortion of the liquid crystalline structure [14].

Magnetic characterization of the samples was performed using a Quantum Design MPMS XL-7 Superconducting Quantum Interference Device (SQUID) magnetometer. Hysteresis curves at 300K were measured for 35% wt HPC in *m*-cresol and for the cobalt ferrite nanoparticles in paraffin, *m*-cresol, and in 35% wt HPC in *m*-cresol. Suspension of the cobalt ferrite particles in paraffin was prepared by mixing the heated (~60^{o}C) paraffin and the particles, which disperse spontaneously, and analyzing them at 300K at which temperature the mixture is solid.

Rheological measurements were performed using an Anton Paar Physica MCR-301 rheometer with plate-plate geometry and a 1mm gap. DC magnetic fields of up to 0.7 T normal to the surface of the plates were applied. During the experiments magnetic field measurements at the sample gap were obtained using a Magnet-Physik FH 54 Gauss-Tesla Meter (Hall Probe) inserted in the bottom stationary plate. Temperature control was achieved using a Julabo

water/ethanol bath and feedback control loop with a thermocouple located also in the stationary bottom plate near the Tesla meter.

6.4 Results and Discussion

Dynamic Light Scattering of the cobalt ferrite particles suspended in *m*-cresol showed a volume average hydrodynamic diameter of approximately 13 nm and a polydispersity of 0.31. This result is in agreement with TEM measurements.

Figure 1 shows the SAXS diffraction pattern for the 15% wt and 35% wt HPC/*m*-cresol samples, both with and without particles. The dotted lines represent samples with suspended cobalt ferrite nanoparticles whereas the solid lines represent samples without magnetic nanoparticles. The appearance of a peak at a scattering vector value of 0.34 $Å^{-1}$ for 35% wt HPC in m-cresol and 0.33 $Å^{-1}$ for 35% wt HPC in *m*-cresol with the cobalt ferrite nanoparticles confirms a liquid crystalline phase. These peaks correspond to correlation lengths of 18 Å (1.8 nm) and 19 Å (1.9nm), respectively. These correlation length values represent a distance between scattering planes, which in our case may be the interpolymeric or pitch distance between each cholesteric twisting HPC.

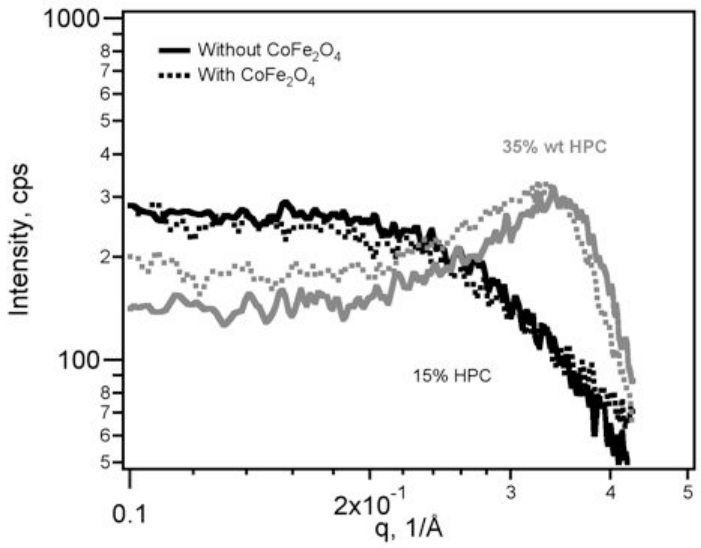

Figure 1. (Gray line) SAXS diffraction pattern for 15 % wt and 35 % wt HPC in *m*-cresol with (dotted lines) and without (solid lines) cobalt ferrite nanoparticles.

Figure 2 shows magnetization curves for suspension of the nanoparticles in paraffin and in *m*-cresol and for 35% wt HPC in *m*-cresol with and without cobalt ferrite nanoparticles. Suspension of the nanoparticles in paraffin confirmed that the particles are magnetically blocked at room temperature, as they show an open hysteresis loop when rotational motion is supressed. It is evident that 35% wt HPC in m-cresol had diamagnetic behavior with no hysteresis prior to suspension of particles, but upon suspension of the cobalt ferrite nanoparticles the liquid crystalline magnetic fluid becomes ferromagnetic, and an open hysteresis loop appears which was not observed with suspension of the particles in *m*-cresol only. Using the ratio of saturation magnetization to domain magnetization, the concentration of the cobalt ferrite nanoparticles in the liquid crystalline matrix was estimated to be 0.007% v/v.

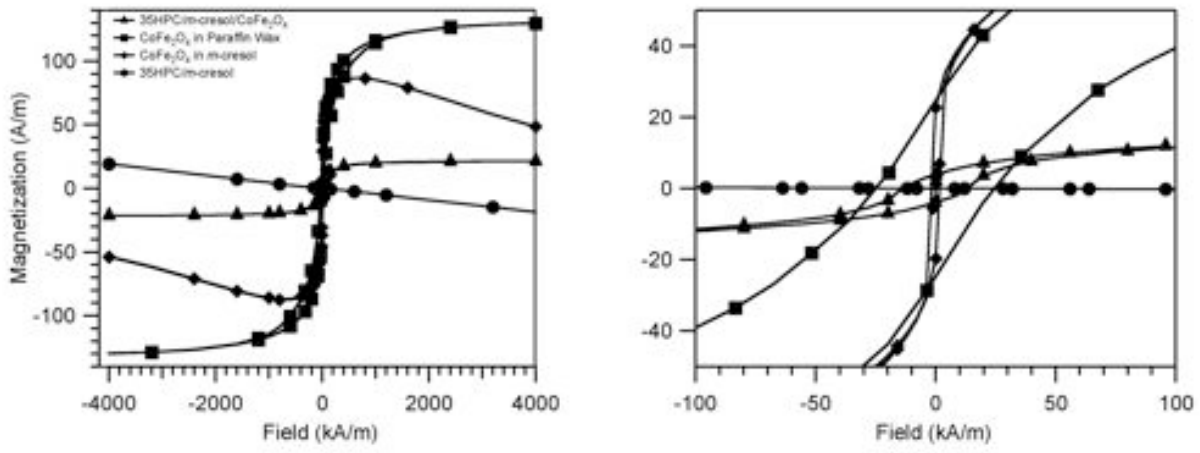

Figure 2. (Left) Equilibrium magnetization for cobalt ferrite nanoparticles in paraffin, *m*-cresol, 35 % wt HPC in m-cresol, and for 35 % wt HPC in *m*-cresol without magnetic content. (Right) Detail of open loops for cobalt ferrite in paraffin and in 35 % wt HPC in *m*-cresol.

Figure 3 shows the magnetically induced enhancement in viscosity (defined as $\Delta\eta=\eta-\eta_{H=0}$) of 15% wt and 35% wt HPC in *m*-cresol with and without particles as a function of applied magnetic field from 0 to 0.7 T and at a constant shear rate of 1 s^{-1}. The viscosity increases as the applied magnetic field increases for samples with and without the magnetic particles. This is an expected result because polymer liquid crystal mesogens may orient in the direction of applied magnetic fields even under flow [12]. The increase in viscosity is more noticeable for the 35% wt HPC in *m*-cresol samples due to the presence of the liquid crystalline phase. The 15% wt HPC sample is a polymer suspension in m-cresol solvent without any orientational or positional order, still it posseses diamagnetic susceptibility which results in orientation of the HPC molecules towards the applied magnetic field. The suspension of cobalt ferrite nanoparticles in 35% wt HPC/*m*-cresol provokes a shift to higher values of viscosity at lower applied magnetic fields. This is akin to the effect of added nanoparticles in decreasing the critical field of the Friederickz transition. In the case of the cobalt ferrite nanoparticles in 15% wt HPC/*m*-cresol no viscosity enhancement is observed because of the low particle concentration and lack of orientational order in the HPC.

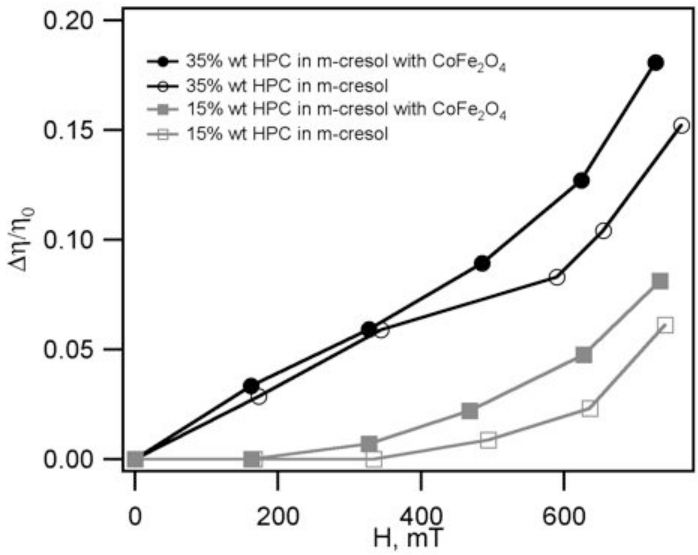

Figure 3. Rheological behavior of 15 % wt HPC in *m*-cresol and 35 % wt HPC in *m*-cresol with and without cobalt ferrite nanoparticles as a function of the applied field and constant shear rate of 1 s^{-1}.

The observed behavior is similar to the magnetoviscous effect observed for commercial ferrofluids [11]. Although this magnetoviscous effect is present with and without the particles, it becomes more evident in the presence of magnetic nanoparticles in the 35% wt HPC/*m*-cresol sample. This is due to the field induced alignment of the magnetic nanoparticles which in effect decreases the magnetic field needed to orient the liquid crystal mesogens in the direction of the applied magnetic field, which is normal to the direction of shear deformation, thereby resisting flow and increasing the viscosity.

6.5 Conclusions

A new type of ferronematic was prepared and characterized showing novel and promising behavior owing to the combination of properties of a conventional ferrofluid and polymer liquid crystals. Suspension of the cobalt ferrite particles did not affect the liquid crystalline phase. However, suspension of the particles did have an effect on the magnetic properties of the medium. 35% wt HPC in *m*-cresol showed diamagnetic behavior without suspended particles, whereas suspension of the particles resulted in ferromagnetic behavior with hysteresis. These particles showed magnetic hysteresis when suspended in paraffin, but not when suspended in *m*-cresol, the latter due to the effect of rotational Brownian motion. These observations indicate that rotational Brownian motion of the particles in 35% wt HPC in *m*-cresol is significantly suppressed.

Magneto-rheology of the samples showed viscosity increments in 15% and 35% wt HPC in *m*-cresol due to an applied magnetic field. This was more evident in the 35% wt sample due to the presence of liquid crystalline order. Viscosity of 35% wt HPC in *m*-cresol increased at lower applied fields upon suspension of cobalt ferrite nanoparticles, whereas no effect was seen in the 15% wt HPC/*m*-cresol/$CoFe_2O_4$ samples, indicating that suspension of particles in the polymer LC phase leads to a decrease in the field needed to orient the mesogens in the direction of the applied magnetic field.

6.6 References

1. Poulin, P., et al., *On the dispersion of latex particles in a nematic solution. I. Experimental evidence and a simple model.* Journal de Physique II, 1994. **4**(9): p. 1557-1569.
2. Hung, F.R., et al., *Nanoparticles in nematic liquid crystals: Interactions with nanochannels.* The Journal of Chemical Physics, 2007. **127**(12): p. 124702.
3. De Gennes, P.G. and J. Prost, *The Physics of Liquid Crsytals*. 2nd ed. 1995, Oxford: Clarendon Press.
4. Kopcanský, P., et al., *The anchoring of nematic molecules on magnetic particles in some types of ferronematics.* Journal of Magnetism and Magnetic Materials Proceedings of the 10th International Conference on Magnetic Fluids, 2005. **289**: p. 101-104.
5. Burylov, S.V. and Y.L. Raikher, *Magnetic Fredericksz transition in a ferronematic.* Journal of Magnetism and Magnetic Materials, 1993. **122**(1-3): p. 62-65.
6. Fokuda, J. and H. Yokoyama, *Stability of the director profile of a nematic liquid crystal around a spherical particle under an external field.* The European Physical Journal E, 2006. **21**(4): p. 341-347.
7. J., C., Y. Haik, and C. Chen, *Biodegradable magnetic gel: synthesis and characterization.* Colloid and Polymer Science, 2003. **281**(9).
8. Tanaka, T., et al., *Collapse of gels in an electric field.* Science, 1982. **218**(29): p. 467-469.

9. Moldenaers, P., et al., *Effect of fillers on the steady state rheological behaviour of liquid crystalline polymers.* Rheologica Acta, 1998. **37**(5): p. 1435-1528.

10. Hartmann, V., et al., *Effects of particles on the steady state and transient rheology of lyotropic hydroxypropylcellulose solutions.* Journal of Rheology, 2000. **44**(6): p. 1417-1432.

11. Odenbach, S., *Magnetoviscous effects in ferrofluids*. 2002, Berlin: Springler.

12. Shufang, F., T. Tomohiro, and C. Shigeomi, *Effect of magnetic field on molecular orientation of nematic liquid crystalline polymers under simple shear flow.* Journal of Rheology, 2008. **52**(2).

13. Shinichi Suto, H.G., Wataru Nishibori, Mikio Karasawa,, *Rheology of liquid crystalline solutions of hydroxypropyl cellulose in m-cresol.* Journal of Applied Polymer Science, 1989. **37**(4): p. 1147-1151.

14. G.D., W., B.K. Annis, and R. Triolo, *X-ray scattering studies of the structure of aqueous hydroxy-propylcellulose solutions.* Journal of Polymer Science. Part B. Polymer Physics, 1991. **29**(3): p. 349-354.

7 Concluding Remarks

This thesis attempted to study the magnetorheology of ferrofluids composed of (i) particles that relax through Neél or Brownian mechanism, (ii) particles having a magnetic field dependent aggregation behavior, (iii) suspensions of minute amounts of particles in a concentrated surfactant solution, and (iv) suspensions of nanoparticles in a crystalline matrix composed of polymeric liquid crystal mesogens.

It was demonstrated that even though Neél and Brownian based FFs show similar magnetoviscous effect, when this response is studied in a dimensionless manner, their behaviors are somewhat dissimilar. This was attributed to the chain formation mechanism that the particles undergo when in contact with an applied external field coupled with the applied external shear deformation, resulting in different hindrance of rotation effect of the Neél and Brownian particles.

We also evidenced the particle aggregation effect on the magnetorheology of FFs having different magnetic field dependent aggregation behavior, where the aggregated FF showed a more pronounced magnetorheological effect with the appearance of a magnetic field induced viscoelastic behavior, not present in the poorly aggregated FF.

Additionally we demonstrated that the rheological behavior of a concentrated surfactant solution may be enhanced by addition of small amounts of magnetic nanoparticles and application of magnetic fields simultaneously. Larger magnetoviscous effect resulted, along with magnetic field dependent yield stresses and viscoelastic behavior. This enhanced rheological behavior also resulted when particles were suspended in a polymeric liquid crystalline matrix, evidencing thus the

reduced magnetic field necessary to align the liquid crystalline mesogens in the direction of the applied magnetic field.

The scientific contributions of this work focused on the magnetorheolgy of FFs studied in terms of their magnetic relaxation, particle-particle interactions and suspending media. With this work we filled an existing gap in the literature where the magnetorheological behavior of FFs has been somewhat misunderstood or attributed to other facts, such as poorly synthesized and polydisperse particles. On the other hand, this work offers up-coming scientists the possibility of investigating new and innovative magnetic materials where the manetorheological response of the fluid may be tuned and/or controlled for specific scientific and/or industrial applications.